Perturbation Methods in the Calculation of Zeeman Interactions and Magnetic Dipole Line Strengths for d^3 Trigonal-Crystal Spectra

R. M. MACFARLANE
Physics Department, Stanford University, Standford, California 94305*
and
IBM Research Laboratory, San Jose, California† 95114
(Received 8 September 1969)

Using a perturbation expansion based on a strong cubic-field zeroth-order approximation, we have obtained analytical expressions for the g values of the t_2^3, $^4A_2$, and ^2F terms for d^3 impurity ions in trigonal crystal fields. We have compared these expressions whth the results of a numerical calculation in which the magnetic dipole operator was transformed to the basis of eigenvectors of the zero-field Hamiltonian computed within the complete d^3 configuration, and we find them to be a very good approximation. This is not true of the published g-value expressions which are currently available. Absolute magnetic dipole absorption cross sections and nonlinear g values are also calculated. This the first time such a detailed calculation of these quantities has been made for transition-ion impurity systems. For levels derived from cubic terms other than t_2^3, $^4A_2$, and ^2E, the analytical-perturbation techniques are not satisfactory and numerical methods must be used. We present an analysis of the g values of the nominally t_2^3 terms, $^4A_2$, ^2E, $^2T_1$, and $^2T_2$, for emerald, ruby, $ZnAl_2O_4:Cr^{3+}$, $MgO:Cr^{3+}$, and $ZnO:Co^{2+}$, and of magnetic dipole absorption cross sections for centrosymmetric $ZnAl_2O_4:Cr^{3+}$ and $MgO:Cr^{3+}$. These systems were chosen because there are quite extensive experimental data available on them. The model parameters were determined from the zero-field energy levels, and very good agreement with experiment was obtained in our calculation of the g values and absorption strengths. This provides confidence in the validity of the crystal-field model to predict the magnetic properties of at least the t_2^3 levels, which couple weakly to phonons.

I. INTRODUCTION

THE response of a magnetic impurity in a diamagnetic host, to either an applied Zeeman field or an oscillating-radiation field, gives important information about the nature of the zero-field eigenstates of the impurity ion and forms a useful starting point for understanding the behavior of the corresponding magnetically concentrated materials. This response has been measured for many d^3 ions present as impurities in crystals, as these have sharp optical and microwave spectra arising from transitions between electronic states which interact only weakly with the lattice. By far, the largest body of data has been obtained on the R line transitions ($^4A_2 \leftrightarrow {}^2E$) and the ground state ($^4A_2$) EPR. For this reason, we will tend to concentrate on these in our analysis.

We report here a numerical calculation of g values, nonlinear Zeeman coefficients, and magnetic dipole (MD) line strengths for some d^3 (and, incidentally, d^7) electronic systems in cubic and trigonal crystal fields. The calculation is exact within the usual crystal-field approximation,[1] i.e., that the impurity orbitals transform like d orbitals under operations of the site symmetry group, and matrix elements between these orbitals and p-like or charge transfer states can be neglected for energy calculations. This static model is a realistic one, as we are primarily interested in levels which are very weakly coupled to the lattice, viz., the nominally t_2^3 levels (Fig. 1). The numerical calculations employ a perturbation expansion based on eigenstates of the complete d^3 zero-magnetic field Hamiltonian, as zeroth-order states. The perturbation is then truly small, viz., the electromagnetic (EM) radiation magnetic field or the static-applied magnetic field. We transform the matrices of L and S to this zeroth-order basis and, hence, obtain linear or nonlinear g values and MD line strengths in a straightforward manner. However, being a numerical method, it requires a new calculation of the zeroth-order eigenstates for each new physical system. Some exploration of the parameter dependence of g values has been carried out, and the whole problem has been programmed for computer processing. The exact numerical solutions have also been used to test the validity of currently used analytical perturbation expressions for g values[2] and MD line strengths.[3,4] In almost every case, they have been found to be inadequate. These analytical expressions use, as zeroth-order states, eigenstates of the cubic-crystal-field term in the Hamiltonian (the so-called "strong-field" approximation). In the case of the $^4A_2$ and ^2E g values, we point out why these expressions are inadequate and extend the previous analytical calculations to provide reasonably accurate working formulas, which show the parameter dependence of the g values explicitly, and which are valid over a reasonably wide range of parameter values (and, hence, physical situations). This complements an analysis of d^3, t_2^3 zero-field splittings (ZFS)

* Work at Stanford University supported by the Army Research Office (Durham) under contract No. ARO-D(208).
† Present address.
[1] Sometimes also called the ligand-field approximation. For a full discussion of this model, see J. S. Griffith, *The Theory of Transition Metal Ions* (Cambridge University Press, Cambridge, England, 1961).
[2] S. Sugano and Y. Tanabe, J. Phys. Soc. Japan **13**, 880 (1958).
[3] S. Sugano, A. L. Schawlow, and F. Varsanyi, Phys. Rev. **120**, 2045 (1960).
[4] G. F. Imbusch, A. L. Schawlow, A. D. May, and S. Sugano, Phys. Rev. **140**, A830 (1965).

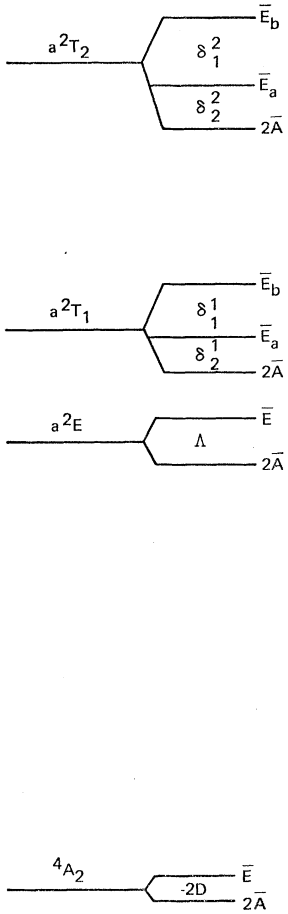

FIG. 1. Schematic energy-level diagram (splittings not to scale) showing to ZFS of the nominally t_2^3 terms.

which was recently carried out.[5] For other cubic terms, it is not practicable to obtain analytical expressions, and one must carry out a detailed numerical calculation. The results of such a calculation are given in Sec. V.

Most of the activity in analyzing d^3 crystal spectra has been concentrated on zero magnetic-field-energy calculations. Sugano and Tanabe[2] were the first to systematically set down perturbation expressions for g values of the t_2^3 terms. Their expressions omit large contributions and were obtained using an unsatisfactory way of dealing with zeroth-order degeneracy. The apparent agreement they obtain in analyzing the ruby g values appears to be fortuitous. Sugano and Peter[6] carried out a numerical calculation for ruby based on a diagonalization of the most important part of the d^3 energy matrix. They chose a fixed ratio between the two trigonal-field parameters ($v'=\frac{1}{3}\sqrt{2}v$), which is accidentally satisfied in ruby but not in most other d^3 systems. We have extended all these g-value calculations and included nonlinear Zeeman interactions and MD line strengths. The present paper also provides a more complete background to a recent analysis of the R-line spectrum of Cr^{3+} in spinels.[7]

[5] R. M. Macfarlane, J. Chem. Phys. **47**, 2066 (1967).
[6] S. Sugano and M. Peter, Phys. Rev. **122**, 381 (1961).

II. DEFINITIONS AND NOTATION

For the case of a d^n impurity ion in a crystal, the zero-field Hamiltonian $\mathcal{H}^{(0)}$ can be written

$$\begin{aligned}\mathcal{H}^{(0)}=&\Delta[-\tfrac{1}{5}(70)^{1/2}U_0^4-2(U_3^4-U_{-3}^4)]\\&+\sum_{i>j}\left[(49B+7C)c_i^{(2)}\cdot c_j^{(2)}+\left(\frac{63}{5}C\right)c_i^{(4)}\cdot c_j^{(4)}\right]\\&+v[-(1/7)(70)^{1/2}U_0^2+(4/21)(70)^{1/2}U_0^4\\&-\tfrac{2}{3}(U_3^4-U_{-3}^4)]+v'[(4/7)(35)^{1/2}U_0^2\\&+(4/7)(35)^{1/2}U_0^4-(2)^{1/2}(U_3^4-U_{-3}^4)]\\&+\zeta\sum_i s_i\cdot l_i\\\equiv&\mathcal{H}_1(\Delta)+\mathcal{H}_2(B,C)+\mathcal{H}_3(v,v')+\mathcal{H}_4(\zeta),\end{aligned}\tag{1}$$

which includes cubic crystal field, single-ion Coulomb, trigonal crystal field, and spin-orbit terms, respectively. The sums over i and j are over individual d-like electrons, and the parametric dependence is shown in the usual notation.[8] $\mathcal{H}^{(0)}$ has the same form for any of the trigonal site groups, viz., D_{3d}, C_{3i}, D_3, C_{3v}, or C_3. This is because the Hamiltonian is time-reversal invariant, and we assume that impurity orbitals transform in the same way as d orbitals under operations of the site group. When an external magnetic field $\mathbf{H}$ is applied to the crystal, it acquires a net moment, and time reversal by itself is no longer a symmetry operation of the site group which will now be one of the magnetic point groups. The Hamiltonian is then

$$\mathcal{H}=\mathcal{H}^{(0)}+\beta\textstyle\sum_\alpha g_\alpha\mu_\alpha H_\alpha,\tag{2}$$

where the g tensor is referred to principal axes and μ is the MD operator. For $\mathbf{H}_{\|}$ c axis, the unitary operations form the subgroup C_3 or C_{3i}, i.e., the possible magnetic symmetry groups[9] are $D_{3d}(C_{3i})$, $C_{3i}(C_{3i})$, $D_3(C_3)$, $C_{3v}(C_3)$, and $C_3(C_3)$. The Zeeman components of the zero-field Kramers's doublets (for $H_{\|}$ c axis) can, therefore, be labeled by the irreducible representations of the unitary double group C_3^*, i.e., $\bar{E}_+$, $\bar{E}_-$, and $\bar{A}$ (or Γ_4, Γ_5, and Γ_6 in Koster's[10] notation). In the absence of the field, $\bar{E}_+$ and $\bar{E}_-$ are degenerate and the $\bar{A}$ levels are degenerate in pairs. The $\bar{E}_+$, $\bar{E}_-$ states are

[7] D. L. Wood, G. F. Imbusch, R. M. Macfarlane, P. Kisliuk, and D. M. Larkin, J. Chem. Phys. **48**, 5255 (1968).
[8] The operators $c^{(2)}$ and $c^{(4)}$, their reduced matrix elements, and the parameters B and C are defined by G. Racah, Phys. Rev. **62**, 438 (1942). For the other parameters, see Ref. 17 and M. H. L. Pryce and W. A. Runciman, Discussions Faraday Soc. **26**, 34 (1958).
[9] In the notation of J. O. Dimmock and R. G. Wheeler, J. Phys. Chem. Solids **23**, 729 (1963).
[10] G. Koster, J. O. Dimmock, R. G. Wheeler, and H. Statz, *Properties of the Thirty-two Point Groups* (The M.I.T. Press Cambridge, Mass., 1963).

composed of linear combinations of $|d^3\alpha SLJM\rangle$ basis states with $M\equiv+\frac{1}{2}, -\frac{1}{2}$ (mod 3). The $\bar{A}$ states have $M\equiv\frac{3}{2}$ (mod 3).

A. g Values

The g value describes the first-order splitting of the $\bar{E}$ and $2\bar{A}$ Kramers' doublets by an external magnetic field. For consistency, it is best defined in terms of an effective spin $S'=\frac{1}{2}$, although for the $^4A_2$ term this may not be quite as convenient as taking $S'=\frac{3}{2}$. We have for the $\bar{E}$ doublets,

$$g_{\parallel}(\bar{E})=2\langle\omega\bar{E}_+|kL_z+g_sS_z|\omega\bar{E}_+\rangle, \tag{3a}$$

$$g_{\perp}(\bar{E})=2\langle\omega\bar{E}_-|kL_x+g_sS_x|\omega\bar{E}_+\rangle, \tag{3b}$$

where $|\omega E_{+,-}\rangle$ are the zero-field eigenstates of $\mathcal{H}^{(0)}$, ω is a label to distinguish different $\bar{E}$ levels, k is the orbital-reduction factor, and g_s is the free-spin g value of 2.0023. The sign of $g_{\parallel}$ is defined to be positive if the $\bar{E}_+$ component has a higher energy than $\bar{E}_-$. No sign is associated with $g_{\perp}$ since the Zeeman components for $\mathbf{H}_{\perp}$ c axis transform according to the same representation of the group C_1*, and the optical and microwave transitions have no polarization properties. The relative sign of the spin and orbital contributions to $g_{\perp}$ is of course, fixed.

For the $2\bar{A}$ doublets, we have a slightly more complicated situation as the two components are labeled by the same representation of C_3*, so that, in general, the computed eigenvectors of $\mathcal{H}^{(0)}$, say $\alpha\bar{A}$ and $\beta\bar{A}$, are not eigenstates of L_z and S_z. Thus,

$$\gamma_a=2\langle\omega,\alpha\bar{A}|kL_z+g_sS_z|\omega,\alpha\bar{A}\rangle, \tag{4a}$$

$$\gamma_b=2\langle\omega,\alpha\bar{A}|kL_z+g_sS_z|\omega,\beta\bar{A}\rangle, \tag{4b}$$

$$g_{\parallel}(2\bar{A})=(\gamma_a^2+\gamma_b^2)^{1/2}, \tag{4c}$$

$$g_{\perp}(2\bar{A})=0 \text{ (by symmetry)}. \tag{5}$$

The states labeled $\alpha\bar{A}$, $\beta\bar{A}$ are arbitrary orthonormal linear combinations of the two components of $2\bar{A}$. There is no straightforward way of attaching a sign to $g_{\parallel}(2\bar{A})$, except perhaps in certain cases by a study of the eigenvectors of $(kL_z+g_sS_z)$. We will take it to be positive. Whereas L_z and S_z are simultaneously diagonalized within $\bar{E}$ by the eigenvectors of the $\mathcal{H}^{(0)}$, this is not true within $2\bar{A}$. This is because the noncommutation of L_z and S_z introduced by spin-orbit coupling does not guarantee simultaneous eigenstates for L_z and S_z. However, for $3d^3$ ions, the spin-orbit interaction is quite small, and it is still possible to separate the contributions of L and S to the g values, to a good approximation. In Sec. V, where the orbital and spin contributions to g are listed separately, it is indiacted that this separation is not rigorous.

B. Nonlinear g Values

In general, g values are only useful for describing first-order Zeeman effects. However, in some simple cases we can describe nonlinear splittings due to interaction between different Kramers' doublets (it being assumed that all Kramers' doublets are separated by the crystal field) by one or two nonlinear g values denoted here by G. Such a nonlinear Zeeman effect has been observed in ruby[11] and emerald[12] using high pulsed magnetic fields. We will consider here the case where only two Kramers' doublets interact via the external field, as this is the situation which has so far been encountered experimentally. For more complicated interactions, it is better to diagonalize a submatrix of the Zeeman interaction. Table I shows which components of $\mathfrak{y}=k\mathbf{L}+g_s\mathbf{S}$ couple the different substates of the Kramers' doublets. We identify a nonlinear G value by the levels which are interacting, e.g., $G_{\parallel}(\alpha\bar{E}_+|\beta\bar{E}_+)=G_{\parallel}(\alpha\bar{E}_-|\beta\bar{E}_-)$ is the nonlinear G value describing the interaction between two $\bar{E}$ doublets for $\mathbf{H}_{\parallel}$ c axis. For this orientation of the external field, nonlinear interactions are only important when two levels belonging to the same zero-field representation have a separation comparable to the magnetic field energy. This could arise, for example, within $^2T_1$, $^2T_2$, $^4T_1$, or $^4T_2$ terms, but not in ^2E or $^4A_2$. The cases of most interest, since they are the only ones measured so far, involve the interaction between $\bar{E}$ and $2\bar{A}$ doublets for $\mathbf{H}_{\perp}$ c axis. This can be described by

$$G_{\perp}(\bar{E}|2\bar{A})=2\langle\bar{E}_+|\mu_x|\bar{A}'\rangle=2\langle\bar{E}_-|\mu_x|\bar{A}''\rangle, \tag{6}$$

where $\bar{A}'$ and $\bar{A}''$ are linear combinations of the components of $2\bar{A}$, such that each one interacts with only one component of $\bar{E}$. For the $t_2^3\,{}^2E$ term, $g_{\perp}(\bar{E})$ is small and can usually be neglected for energy calculations. In this case, we can write the energies of the two doubly degenerate levels as[11]

$$E_{1,2}=\pm\tfrac{1}{2}\{\Lambda_0^2+[G_{\perp}(\bar{E}|2\bar{A})\beta H]^2\}^{1/2}, \tag{7}$$

where Λ_0 is the ZFS between $\bar{E}$ and $2\bar{A}$. If $g_{\perp}(\bar{E})$ cannot be neglected, the Zeeman matrix must be numerically diagonalized within the four substates, and four nondegenerate components are obtained. Thus, although $g_{\perp}(2\bar{A})$ is zero, the $2\bar{A}$ level may still split via a nonlinear interaction with components of $\bar{E}$. Although they do not make the distinction, this is in fact what Sugano and Peter[6] calculated when they reported a nonvanish-

TABLE I. Selection rules for components of the MD operator in trigonal symmetry. Alternative representation labels are given and these are defined in the text.

	Γ_4 $\bar{E}_+$	Γ_5 $\bar{E}_-$	Γ_6 $\bar{A}$
$\Gamma_4\,\bar{E}_+$	μ_z	μ_+	μ_-
$\Gamma_5\,\bar{E}_-$	μ_-	μ_z	μ_+
$\Gamma_6\,\bar{A}$	μ_+	μ_-	μ_z

[11] K. Aoyagi, A. Misu, and S. Sugano, J. Phys. Soc. Japan **18**, 1448 (1963).
[12] D. L. Wood, J. Chem. Phys. **42**, 3404 (1965).

ing $g_\perp$ for the $2\bar{A}$ level of $a\,^2E$. Nonlinearity in the $^4A_2$ Zeeman splittings for $\mathbf{H}_\perp$ c axis is very pronounced because the ZFS are small ($\sim$1 cm^{-1}). However, for $3d^3$ ions, the departure from the free-spin g value is small, and we have the approximate relationship

$$G_\perp(E|2A)\approx\sqrt{3}g_\perp(E) \quad \text{for} \quad {}^4A_2. \tag{8}$$

For a typical $3d^3$ ion, this relationship is good to 1 part in 10^5, and must be satisfied if the EPR spectrum is to fit an $S=\frac{3}{2}$ spin Hamiltonian with a single g value. When orbital admixture into $^4A_2$ is relatively large, as, for example, in $5d$ ions or tetrahedrally coordinated Co^{2+}, Eq. (8) may no longer hold and two independent g values will be required. For example, for Re^{4+} ($\zeta\approx 2000$ cm^{-1}), we find approximately a 20% departure from the relation (8).

C. MD Intensities

MD transitions are usually only observed in cases where the impurity ion is at a center of symmetry, as there is then no odd-parity crystal-field component to allow the stronger ED transitions. We will, therefore, be concerned with the zero-phonon lines of impurity ions in O_h, D_{3d}, or C_{3i} sites as, for example, for Cr^{3+} in MgO, spinels, or garnets, respectively. Since MD transitions are parity-allowed within d^n configurations, absolute intensities can be calculated in a relatively straightforward manner. At most, we need only take account of spin-orbit mixing in order to get a nonvanishing transition matrix element. In addition, in paramagnetic systems, MD intensities are not subject to uncertain effective field corrections. The quantities which we directly calculate are line strengths. These can be defined by analogy with corresponding free-ion quantities.[13] Thus, we have, for transitions between nondegenerate components,

$$\begin{aligned}\mathcal{S}_\kappa(\alpha S\Gamma\Gamma_T\gamma_T;\alpha S'\Gamma'\Gamma_T'\gamma_T')\\ =|\langle\alpha S\Gamma\Gamma_T\gamma_T|\beta\mu_\kappa e_\kappa|\alpha' S'\Gamma'\Gamma_T'\gamma_T'\rangle|^2\end{aligned} \tag{9}$$

where κ labels the components of the MD operator $\mathfrak{y}=(k\mathbf{L}+g_s\mathbf{S})$ and $\mathbf{e}$ is the unit vector expressing the polarization of the radiation, (i.e., we define the transition line strength for a particular component of the incident radiation field). For transitions between unsplit Kramers' doublets $\hat{\Gamma}_T$, it is useful to define

$$\begin{aligned}\mathcal{S}_\kappa(\alpha S\Gamma\hat{\Gamma}_T;\alpha' S'\Gamma'\hat{\Gamma}_T')\\ =\sum_{\hat{\gamma}_T\hat{\gamma}_T'}\mathcal{S}_\kappa(\alpha S\Gamma\hat{\Gamma}_T\hat{\gamma}_T;\alpha' S'\Gamma'\hat{\Gamma}_T'\hat{\gamma}_T'),\end{aligned} \tag{10}$$

or, for transitions between cubic terms,

$$\mathcal{S}_\kappa(\alpha S\Gamma;\alpha' S'\Gamma')=\sum_{\hat{\Gamma}_T\hat{\Gamma}_T'}\mathcal{S}_\kappa(\alpha S\Gamma\hat{\Gamma}_T;\alpha' S'\Gamma'\hat{\Gamma}_T'). \tag{11}$$

[13] E. U. Condon and G. H. Shortley, *The Theory of Atomic Spectra* (Cambridge University Press, Cambridge, England, 1935).

Six other quantities involving pairs of the labels $\hat{\gamma}_T$, $\hat{\Gamma}_T$, and $S\Gamma$ can be defined in a similar way. Which one is appropriate to use depends on which degeneracies have been lifted and whether component lines are resolved.

For many purposes, it is convenient to define a line strength in which the Bohr magneton ($e\hbar/2mc$) has been factored out, i.e.,

$$\mathcal{S}_\kappa'=(1/\beta^2)\mathcal{S}_\kappa, \tag{12}$$

so that $\mathcal{S}_\kappa'$ comprises just matrix elements of $\mathbf{L}$ and $\mathbf{S}$, which for allowed transitions are of the order of unity, in units of $\hbar$. It remains to relate the line strengths defined above to quantities which are directly measured, for example, the integrated absorption coefficient per ion, the oscillator strength, and the radiative lifetime. These relationships are explored further in Appendix A. We give here useful expressions for the case of MD R lines ($t_2^3\,{}^2E\leftrightarrow{}^4A_2$), in which the ground-state components are optically resolved (i.e., there are four R lines). We also assume here that the ground-state splitting is much smaller than kT, so that the two components of $^4A_2$ have equal populations (for cases when this is not true see Appendix A). The integrated absorption coefficient per atom for one of the R lines, for a given polarization κ, is

$$\begin{aligned}\left(N^{-1}\int k_\sigma d\sigma\right)_\kappa(^2E\hat{\Gamma}_T;{}^4A_2\hat{\Gamma}_{T'})=2.685\times10^{-23}\eta\sigma\\ \times\mathcal{S}_\kappa'(^2E\hat{\Gamma}_T;{}^4A_2\hat{\Gamma}_{T'})\text{ cm},\end{aligned} \tag{13}$$

where σ is the energy of the transition in cm^{-1}, k_σ is the absorption coefficient at the energy σ, and η is the refractive index of the crystal. Expressions for the other three lines follow trivially by substituting an S' with the appropriate $\hat{\Gamma}_T$, $\hat{\Gamma}_{T'}$. If the ground-state splitting is not resolved, a summation over the components can be carried out. For the two most common line shapes, we can set

$$\begin{aligned}N^{-1}\int k_\sigma\,d\sigma&=\frac{1}{2N}\left(\frac{\pi}{\ln 2}\right)^{1/2}k_{\max}\Delta\sigma\text{ cm (Gaussian)},\\ N^{-1}\int k_\sigma\,d\sigma&=\frac{1}{2N}\pi k_{\max}\Delta\sigma\text{ cm (Lorentzian)},\end{aligned} \tag{14}$$

where $k_{\max}$ is the peak-absorption coefficient and $\Delta\sigma$ is the linewidth.

Equations (13) and (14) summarize the important expressions needed to relate the peak-absorption coefficient and half-width to the matrix elements of $\mathbf{L}$ and $\mathbf{S}$. The oscillator strength, a derived quantity of largely historical interest, is given by

$$f_\kappa=1.1297\times10^{12}\frac{1}{\eta}\left(N^{-1}\int k_\sigma\,d\sigma\right)_\kappa, \tag{15}$$

and the radiative lifetime τ_r at 0°K is given by

$$\tau_r^{-1}=2.6971\times10^{-11}\eta^3\sigma^3 \times\tfrac{1}{2}\sum_\kappa \mathcal{S}_\kappa'({}^4A_2;{}^2E\hat{\Gamma}_{T'})\ \text{sec}^{-1}, \quad (16)$$

where $\hat{\Gamma}_T$ is the lower component of ^2E. The lifetime will change as a function of temperature if the line strength from the upper ^2E component (i.e., R_2) is different from the lower one (R_1). If we average over the two R line lifetimes, a useful expression is

$$\tau_r^{-1}({}^4A_2,{}^2E)=0.75\times10^{-10}\eta^2\sigma^2 \times\tfrac{1}{3}\sum_\kappa\left(\frac{1}{N}\int k_\sigma\, d\sigma\right)_\kappa({}^2E,{}^4A_2)\times10^{22}\ \text{sec}^{-1}. \quad (17)$$

III. NUMERICAL CALCULATIONS

It will be convenient to outline here the steps in the numerical calculation of both g values and MD line strengths, as these are closely related. We start with the time-independent zeroth-order zero-field Hamiltonian $\mathcal{H}^{(0)}$ [Eq. (1)] which includes Coulomb, trigonal crystal field, and spin-orbit terms. Matrix elements of $\mathcal{H}_0$ were calculated in a "weak-field" $|\alpha SLJM\rangle$ basis for the complete d^3 configuration, as described in an earlier paper.[14] For a choice of real basis functions, the matrix of $\mathcal{H}^{(0)}$ factorizes into three blocks (labeled by the epresentations $\bar{E}_+$, $\bar{E}_-$, and $2\bar{A}$) for which $M\equiv\frac{1}{2}$ (mod 3), $-\frac{1}{2}$ (mod 3), and $\frac{3}{2}$ (mod 3), respectively. For C_{3v}, D_3, or D_{3d} symmetries, the $2\bar{A}$ block could be further factored into two subblocks by choosing a complex basis (which yields complex matrix elements), but it was more convenient for computation to retain the real form. In any case, the complex basis does not diagonalize L_z or S_z and so is not a convenient choice for g-value calculations. The transformation from the "calculation basis" $|\alpha SLJM\rangle$ to the symmetry basis for the problem, i.e., $|\alpha SLJ\hat{\Gamma}_T\hat{\gamma}_T\rangle$ where $\hat{\Gamma}_T\hat{\gamma}_T$ label representations and components of C_3*, is only a simple change of phase. The zero-order Hamiltonian $\mathcal{H}^{(0)}$ consists of six matrices of order 39 for each of $\bar{E}_+$ and $\bar{E}_-$ and six of order 42 for $2\bar{A}$. These were made up of three crystal-field matrices (coefficients of A_0^2, A_0^4, and A_3^4, or, equivalently, Δ, v, v'), two Coulomb matrices (coefficients of the Racah parameters B and C), and one spin-orbit matrix (coefficient of ζ).

We now outline the calculation of the magnetic-perturbation terms. The MD operator $\mathfrak{y}=(k\mathbf{L}+g_s\mathbf{S})$ is diagonal in S and L and satisfies the triangular selection rules $(J,1,J')$ and $(M,1,M')$ on J and M. It is desirable to calculate matrix elements of $\mathbf{L}$ and $\mathbf{S}$ separately rather than express $\mathbf{L}+2\mathbf{S}=\mathbf{J}+\mathbf{S}$, which would otherwise be convenient, as the matrix of $\mathbf{J}$ is diagonal in the quantum number J. One can then evaluate the spin and orbital contributions to g values separately and make allowance for partial quenching of the orbital contribution by covalency or Jahn-Teller effects.[15] Relatively simple closed expressions can be written for the matrix elements of $k\mathbf{L}$ and $g_s\mathbf{S}$, where k is the orbital-reduction factor and g_s is the free-spin g value=2.0023. These expressions depend only on the quantum numbers S, L, J, and M and, hence, are valid for any l^n configuration.

$$\begin{aligned}
&\langle\alpha SLJM|kL_z+g_sS_z|\alpha SLJM\rangle=[k+(g_s-k)K_1]M,\\
&\langle\alpha SLJM|kL_z+g_sS_z|\alpha SLJ-1M\rangle\\
&\qquad=(g_s-k)K_2[(J+M)(J-M)]^{1/2},\\
&\langle\alpha SLJM|kL_x+g_sS_x|\alpha SLJM-1\rangle\\
&\quad=\tfrac{1}{2}[(g_s-k)K_1+k][(J-M+1)(J+M)]^{1/2},\\
&\langle\alpha SLJM|kL_x+g_sS_x|\alpha SLJ-1M-1\rangle\\
&\qquad=-\tfrac{1}{2}(g_s-k)K_2[(J+M-1)(J+M)]^{1/2}, \quad (18)\\
&\langle\alpha SLJ-1M|kL_x+g_sS_x|\alpha SLJM-1\rangle\\
&\qquad=\tfrac{1}{2}(g_s-k)K_2[(J-M)(J-M+1)]^{1/2},
\end{aligned}$$

where

$$\begin{aligned}
K_1&=[J(J+1)+S(S+1)-L(L+1)]/2J(J+1),\\
K_2&=[(S+L+J+1)(L+J-S)(S+J-L)\\
&\quad\times(L+S-J+1)]^{1/2}/[4J^2(2J-1)(2J+1)]^{1/2}.
\end{aligned}$$

We have used these expressions to calculate matrix elements of kL_z and g_sS_z, for the $\bar{E}_-$ and $2\bar{A}$ blocks, and of kL_x and g_sS_x, for the $\bar{E}_-/\bar{E}_+$ and $\bar{E}_-/2\bar{A}$ blocks.

A 7090 FORTRAN IV program was written to carry out the numerical steps as follows. A linear combination of the six zero-field matrices with given values of Δ, v, v', B, C, and ζ, for each representation, was diagonalized and the eigenvectors computed. The eigenvalue/eigenvector subroutine used the Jacobi algorithm, as it is simple and readily gives orthogonal vectors for degenerate eigenvalues. The $2\bar{A}$ matrix has the form

$$\begin{bmatrix} A & -B \\ B & A \end{bmatrix},$$

where A is a real symmetric matrix and B is a real skew symmetric. No attempt was made to utilize this symmetry, although the Householder algorithm has been adapted[16] to operate directly on the equivalent complex Hermitian form $A+iB$. One compensation for our lack of sophistication was that the double degeneracy of the $2\bar{A}$ eigenvalues provided a check on the significance of the eigenvalues which was found to be eight figures. The diagonal elements of the six zero-field matrices for each representation were computed in a basis of the eigenvectors of $\mathcal{H}^{(0)}$. This gave the first-order dependence of the zero-field levels on the parameters Δ, v, v', B, C, and ζ, and also provided an identification label for the levels when components of different cubic terms overlapped.

[14] R. M. Macfarlane, J. Chem. Phys. **39**, 3118 (1963).

[15] K. W. H. Stevens, Proc. Roy. Soc. (London) **A219**, 542 (1953); F. S. Ham, Phys. Rev. **138**, A1727 (1965).

[16] D. J. Mueller, Numerische Mathematik **8**, 72 (1966).

The second part of the program transformed the matrices of L_z, S_z, L_x, and S_x to the basis of the eigenvectors of $\mathcal{H}^{(0)}$. The output consisted of eight matrices: L_z and S_z for $\bar{E}_-$ and $2\bar{A}$, and L_x, S_x for $\bar{E}_-/\bar{E}_+$ and $\bar{E}_-/2\bar{A}$. This provided all of the matrix elements required by Eqs. 3–6, (9), and (13). More recently, this program has been run on a 360/91 computer using double-precision arithmetic.

IV. ANALYTICAL PERTURBATION APPROXIMATION

Ideally, we would like analytical expressions for the g values and MD line strengths in terms of the model parameters. However, since the individual terms of $\mathcal{H}$ [Eq. (2)] do not commute, it is not possible to find a basis which simultaneously diagonalizes them for arbitrary values of the model parameters. The only way to obtain analytical expressions (and these will be approximate) is to use a perturbation expansion based on a suitable zeroth-order Hamiltonian $H^{(0)}$. In the numerical calculations of Sec. III, only the Zeeman term was treated as a perturbation, i.e., $H^{(0)}\equiv\mathcal{H}^{(0)}$. For analytical expressions, however, (as we have pointed out before in a discussion of ZFS[5]) the best choice we can make for $H^{(0)}$ in situations of near-cubic symmetry is

$$H^{(0)}=\mathcal{H}_1(\Delta)+\mathcal{H}_2{}^a(B,C)\,, \tag{19}$$

where $\mathcal{H}_2{}^a(B,C)$ is the diagonal part of the Coulomb interaction in a basis which diagonalizes $\mathcal{H}_1(\Delta)$ (i.e., the strong cubic-field basis). This removes diagonal Coulomb interactions from the perturbation and puts into zeroth-order terms which would have occurred in an infinite number of higher orders had we chosen $\mathcal{H}_1(\Delta)$ to be $H^{(0)}$. Our zeroth-order eigenstates are now the cubic eigenstates $|t_2{}^m(S_1\Gamma_1)e^n(S_2\Gamma_2)S\Gamma M_s\gamma\rangle$ and we must express the matrix elements of $\mathcal{H}$ in this basis. It is, therefore, convenient to express $\mathcal{H}$ [Eqs. (1a) and (1b)] in terms of cubic tensor operators,[17] rather than the spherical tensors of Eqs. (1a) and (1b). The techniques for calculating the matrix elements of $\mathcal{H}$ in the strong cubic-field basis has been treated thoroughly by Tanabe and co-workers[17] and by Griffith.[1,18] Instead of using the full cubic-term labels, we make the notational abbreviation introduced by Sugano and Peter[6] and used by the author[5] (see Table II). We use the Rayleigh-Schrödinger expansion[19] of the eigenvalues of the perturbation Hamiltonian $P=\mathcal{H}-H^{(0)}$. The convergence of the perturbation expansion depends, of course, on the relative sizes of the parameters describing each term of $\mathcal{H}$. We wish to investigate whether good approximations to g values and MD line strengths can be obtained by considering a limited number of perturbation loops. Only the cases of $g(^4A_2)$ and $g(a^2E)$ will be considered in detail, as these are the ones most commonly measured and, hence, for which most data are available. We note that although there are no first-order ZFS of the half-filled shell $t_2{}^3$ cubic terms, there are first-order Zeeman splittings.

TABLE II. Energy denominators in zeroth order.

$$D_1=W(^4T_2)-W(^4A_2)=\Delta$$
$$D_2=W(a\,^2T_2)-W(^4A_2)=15B+4C$$
$$D_3=W(b\,^2T_2)-W(^4A_2)=\Delta+9B+3C$$
$$D_4=W(a\,^4T_1)-W(^4A_2)=\Delta+12B$$
$$D_7=W(a\,^2T_2)-W(a\,^2E)=\Delta+6B$$
$$D_8=W(b\,^2T_1)-W(a\,^2E)=\Delta+6B$$
$$D_9=W(b\,^2T_2)-W(a\,^2E)=\Delta$$
$$D_{10}=W(c\,^2T_1)-W(a\,^2E)=\Delta$$
$$D_{11}=W(c\,^2T_2)-W(a\,^2E)=\Delta+10B$$
$$D_{12}=W(b\,^2E)-W(a\,^2E)=\Delta+14B+3C$$
$$D_{13}=W(c\,^2E)-W(a\,^2E)=\Delta+5B$$
$$D_{14}=W(^4T_2)-W(a\,^2E)=\Delta-9B-3C$$

where

$a\,^2E\equiv t_2{}^3\,^2E$	$a\,^2T_1\equiv t_2{}^3\,^2T_1$	$a\,^2T_2\equiv t_2{}^3\,^2T_2$
$b\,^2E\equiv t_2{}^2(^1A_1)e\,^2E$	$b^2T_1\equiv t_2{}^2(^3T_1)e\,^2T_1$	$b\,^2T_2\equiv t_2{}^2(^3T_1)e\,^2T_2$
$c\,^2E\equiv t_2{}^2(^1E)e\,^2E$	$c^2T_1\equiv t_2{}^2(^1T_2)e\,^2T_1$	$c\,^2T_2\equiv t_2{}^2(^1T_2)e\,^2T_2$

A. Ground-Term g Values

The g values of the $\bar{E}$ component of the $^4A_2$ ground term deviate by a small, though accurately measurable, amount from the spin-only value $g_s=2.0023$. The g values of the $2\bar{A}$ component [as defined by Eq. (3)] follow the spin-only relationship

$$g_{\parallel}(2\bar{A})=3g_{\parallel}(\bar{E})\,, \tag{20}$$

and also Eq. (8), to about 1 part in 10^5 for octahedral Cr^{3+} systems. As noted earlier, measurable departure from these relationships occurs only in cases of large spin-orbit coupling (e.g., in $5d$ ions) or when the cubic crystal field is very weak. We will, therefore, concentrate our discussion on $g(\bar{E})$. Because the $^4A_2$ term is separated by about 10 000 cm^{-1} from the next excited term, we have confidence that the convergence of the perturbation expansion of its splittings will be good. In fact, of all the ZFS of d^3 terms, that of $^4A_2$ can most reliably be approximated by perturbation expressions.[5]

We now enumerate the contributions to $g_{\parallel}$ and $g_{\perp}$. All perturbation loops to third order which give rise to a magnetic-splitting linear in the applied field are shown in Fig. 2. To first order (loop *i*), g is isotropic and spin-only. The second-order contribution (loop *ii*) is orbital, isotropic, and about two orders of magnitude down on first order. In third order, there are two main mechanisms: The first (loops *iii–ix*) produces small isotropic corrections to g, and the second and more important (loops *x–xii*) gives rise to anisotropy in the

[17] Y. Tanabe and S. Sugano, J. Phys. Soc. Japan **9**, 753 (1954); Y. Tanabe and H. Kamimura, *ibid.* **13**, 394 (1958).
[18] J. S. Griffith, *The Irreducible Tensor Method for Molecular Symmetry Groups* (Prentice-Hall International, London, 1962).
[19] A. Messiah, *Quantum Mechanics* (North-Holland Publishing Co., Amsterdam, 1962), Chap. 16.

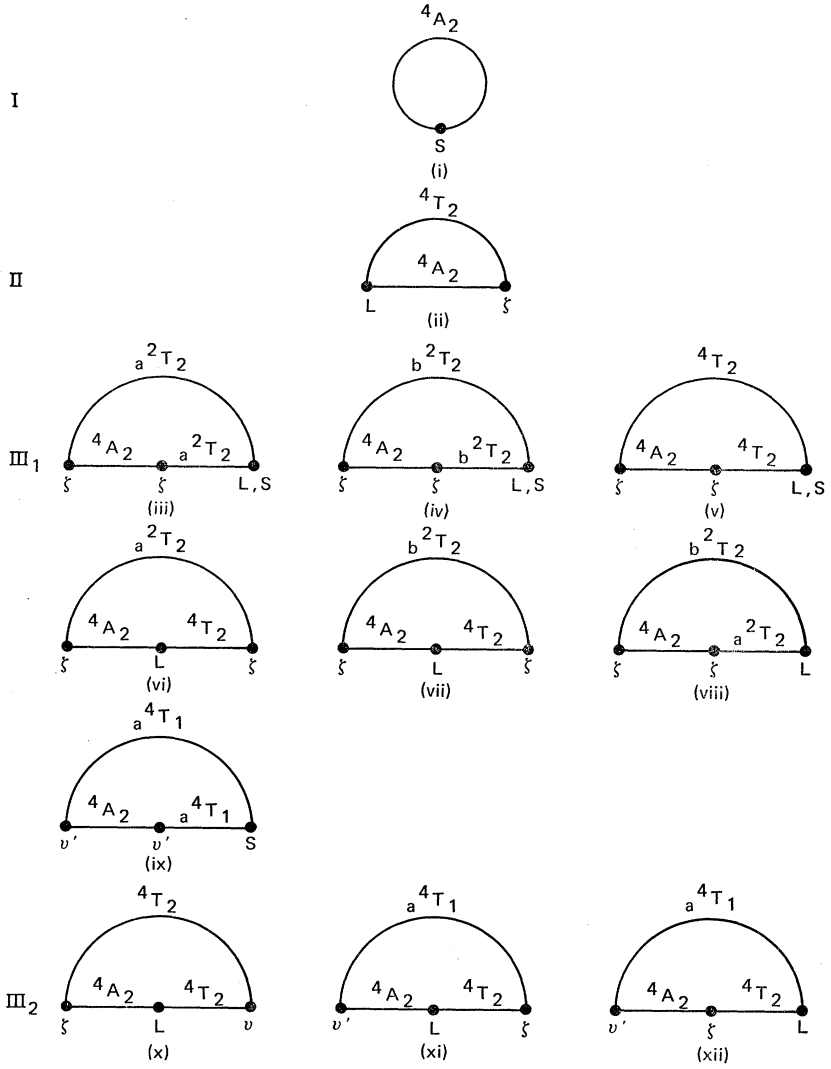

FIG. 2. Perturbation loops, linear in the Zeeman interaction, which contribute to the g values of the $^4A_2$ ground state to third order. The third-order loops labeled III_1 contribute equally to $g_\parallel$ and $g_\perp$ and those labeled III_2 contribute to the g-value anisotropy $g_\parallel - g_\perp$.

g value. The analytical expressions for these are

$$g_\parallel^{(1)} = g_\perp^{(1)} = g_s ,$$

$$g_\parallel^{(2)} = g_\perp^{(2)} = -(8\zeta/3D_1)k ,$$

$$g_\parallel^{(3)} - g_\perp^{(3)} = (4\zeta v/3D_1^2)k - (4\sqrt{2}\zeta v'/D_1D_4)k ,$$

$$g_\parallel^{(3)} = \Big(-\frac{2\zeta^2}{3D_2^2}(k+g_s) + \frac{4\zeta^2}{9D_3^2}(k-2g_s) + \frac{8\zeta^2}{9D_1^2}(k-2g_s) - \frac{4\zeta^2}{3D_1D_2}k + \frac{4\zeta^2}{9D_1D_3}k + \frac{4\zeta^2}{3D_2D_3}k \Big) + \frac{8\zeta v}{9D_1^2}k - \frac{8\sqrt{2}\zeta v'}{3D_1D_4}k , \quad (21)$$

where the energy denominators are given in Table II.

The part of $g_\parallel^{(3)}$ in large parantheses does not contribute to the anisotropy of g (i.e., $g_\perp^{(3)}$ contains the same terms) and for most practical purposes is negligible compared to the second-order contribution. The ratio of the g-value anisotropy to its departure from g_s is $\frac{1}{2}[(3\sqrt{2}v'/D_4) - (v/D_1)]$. This is independent of ζ and k and, so, is a good quantity to compare from ion to ion in an isoelectronic series, for example. The g-value anisotropy is predominantly proportional to v', as is the ZFS $D(^4A_2)$. [We have defined[5] $D(^4A_2)$ in such a way that it is equal to $-2D$ of the conventional spin Hamiltonian.] Thus, we can say qualitatively that, when the $2\bar{A}$ component of $^4A_2$ lies lowest, $g_\parallel$ will almost always be less than $g_\perp$.[20] The actual relationship between $(g_\parallel - g_\perp)$ and $D(^4A_2)$ is rather complicated, as can be seen by comparing Eq. (21) with Table I of Ref. 5. Attempts to explain the approximate proportionality

[20] For Cr^{3+}, systems this is always observed to be the case, experimentally. However, the difference $(g_\parallel - g_\perp)$ is small, usually less than 0.002, so there is a large uncertainty in its measurement.

between $(g_{\parallel}-g_{\perp})$ and $D(^4A_2)$ have been made before[21] using a single-perturbation loop linear in v (i.e., $^4A_2-^4T_2$ interactions only). However, this predicts a proportionality constant which is too small, and it gives the wrong sign for both $(g_{\parallel}-g_{\perp})$ and $D(^4A_2)$.

B. a^2E g Values

The four substates of ^2E have the M_s and γ quantum numbers $\pm\frac{1}{2}u_{\pm}$, where u_+, u_- are components of E in trigonal quantization. Now $-\frac{1}{2}u_+$ and $\frac{1}{2}u_-$ transform irreducibly according to different one-dimensional complex-conjugate representations of the double group C_3*, which is the appropriate symmetry group for $\mathbf{H}_{\parallel}$ c axis. These two substates are, therefore, eigenstates of L_z and S_z. On the other hand, $\frac{1}{2}u_+$ and $-\frac{1}{2}u_-$ are eigenstates of the crystal-field Hamiltonian $\mathcal{H}^{(0)}$, but not of L_z and S_z [see the definition of $2\bar{A}$ g values in Eqs. (4) and (5)]. When $\mathbf{H}$ is parallel to the c axis, there is no interaction between $\bar{E}$ and $2\bar{A}$ components and, hence, no nonlinear $G_{\parallel}$ within ^2E.

In first order, there is no orbital contribution to $g(^2E)$, so $g_{\parallel}{}^{(1)}(\bar{E})$ and $g_{\parallel}{}^{(1)}(2\bar{A})$ both have the values g_s. In second and higher orders, the orbital contributions produce departures from g_s which, for Cr^{3+} systems, are typically 25–50%, but they may be even larger than this (as, for example, in $ZnAl_2O_4:Cr^{3+}$). Sugano and Tanabe[2] have given an expression for g by considering second-order perturbations within the t_2^3 configuration. We show that the apparent agreement they obtained with the measured g values in ruby was fortuitious, and that it is, in fact, difficult to obtain a strongly convergent analytical expansion for the $a\,^2E$ g values. The reason for this is that there is a Zeeman interaction between the $a\,^2E$ and $a\,^2T_1$ terms which are degenerate in zeroth order [zeroth order being defined by Eq. (19)]. Sugano and Tanabe[2] got around this by replacing the resonant denominator by the experimental energy separation $W(a\,^2T_1')-W(a\,^2E')$,[22] (the primes indicating that these are no longer zeroth-order states) a procedure also used later by Clogston[23] in his calculation of $g_{\perp}(E)$. However, this method gives poor convergence as there is still a quasidegeneracy between $a\,^2E'$ and $a\,^2T_1'$, in the sense that off-diagonal matrix elements of the Coulomb and trigonal-field perturbations are comparable in magnitude (500–1000 cm^{-1}) to the separation $W(a\,^2T_1')-W(a\,^2E')$.[24] In addition, by not considering interactions outside of the t_2^3 configuration, Sugano and Tanabe neglected contributions to the g values which are several times larger than those within t_2^3.

To deal with the zeroth-order degeneracy, we must diagonalize the perturbations within the degenerate $a\,^2E$, $a\,^2T_1$ manifold. In general, this would give rise to numerical solutions, but as we now show, we can get useful, though rather clumsy, analytical expressions which can be evaluated on a desk calculator.

We first of all break the perturbation Hamiltonian $\mathcal{H}-H^{(0)}$ into zero-field and Zeeman parts. For the orbital part of the g value, the important Zeeman term is that connecting $a\,^2E$ and $a\,^2T_1$. We then compute the matrix of $P=\mathcal{H}-H^{(0)}$ within $a\,^2E$, $a\,^2T_1$ for $\bar{E}$ and $2\bar{A}$ to second order (denoted$^{(2)}$) in the zero-field perturbations, considering interactions with all d^3 excited states $|\alpha\bar{S}\bar{\Gamma}\bar{M}_s\bar{\gamma}\rangle$. This gives

$$\langle{}^2\Gamma M_s\gamma|P|{}^2\Gamma' M_s'\gamma'\rangle^{(2)}\equiv-\sum_{\bar{S}\bar{\Gamma}\bar{M}_s\bar{\gamma}}\frac{\langle{}^2\Gamma M_s\gamma|P|\alpha\bar{S}\bar{\Gamma}\bar{M}_s\bar{\gamma}\rangle\langle\alpha\bar{S}\bar{\Gamma}\bar{M}_s\bar{\gamma}|P|{}^2\Gamma' M_s'\gamma'\rangle}{W(\bar{\Gamma})-W(\Gamma)},\tag{22}$$

where $^2\Gamma$, $^2\Gamma'$ denote $a\,^2E$ and/or $a\,^2T_1$ and the W's are diagonal elements of the zeroth-order Hamiltonian $H^{(0)}$ [Eq. (19)].

There are 52 perturbation loops contributing to the diagonal and off-diagonal elements of Eq. (22). These will not be shown explicitly because there are so many and because the physical mechanisms corresponding to the loops are not as apparent as in the case of the $^4A_2$ g values. The individual matrix elements on the right-hand side of Eq. (22) were calculated using standard techniques[17,18] of the cubic tensor operator formalism. The resulting nonvanishing zero-field matrix elements on the left-hand side are designated in Table III by the λ's and κ's and expressions for the latter are given in Appendix B. An inspection of these expressions shows that the dominant contributions arise from Coulomb and trigonal (via v') admixtures of t_2^2e, ^2E, and $^2T_1$ terms. This contrasts with the t_2^3 mechanism of Sugano and Tanabe.[2]

The next step is to diagonalize the $\bar{E}$ and $2\bar{A}$ matrices of the zero-field perturbation (i.e., the λ and κ part of Table III), yielding eigenvectors $\langle{}^2\Gamma M_s\gamma|{}^2E\bar{E}\rangle$ and $\langle{}^2\Gamma M_s\gamma|{}^2E2\bar{A}\rangle$ with $^2\Gamma$ referring to the rows of the matrices in Table III. The Zeeman matrix is then transformed to this basis to yield g values in accordance with the definitions of Eqs. (3)–(5). At this stage we note two simplifications.

(i) The diagonalization of the 4×4 $2\bar{A}$ matrix can be simplified by transforming it into two 2×2's by taking

[21] See, for example, W. Low, *Paramagnetic Resonance in Solids* (Academic Press Inc., New York, 1960), where the expression $D=\frac{1}{6}\zeta(g_z-g_x)$ is given.

[22] At best, this is equivalent to taking the energy denominators to a higher order than the basis states in which the perturbation matrix elements are expressed.

[23] A. M. Clogston, Phys. Rev. **118**, 1229 (1960).

[24] This does not, of course, arise in the case of our exact numerical solution, as the perturbation is then just the Zeeman term which is truly small compared to this separation.

TABLE III. Matrices of the perturbation operator $\mathcal{H}-H^{(0)}$ for $\mathbf{H}_{\perp c}$ within the degenerate a^2E, a^2T_1 manifold. Detailed expressions for the λ's and κ's are given in Appendix B. The $\bar{E}_-$ matrix is equal to that given for $\bar{E}_+$ and all are real Hermitian.

	$a\,^2E^{(2)}$		$a\,^2T_1{}^{(2)}$	
$\bar{E}_+$	$-\frac{1}{2}u_+$		$-\frac{1}{2}a_+$	$\frac{1}{2}a_0$
$-\frac{1}{2}u_+$	$\lambda_1-\frac{1}{2}g_s$			
$-\frac{1}{2}a_+$	$\lambda_2+\sqrt{2}k$		$\lambda_3+k-\frac{1}{2}g_s$	
$\frac{1}{2}a_0$	λ_4		λ_5	$\lambda_6+\frac{1}{2}g_s$
	$a\,^2E^{(2)}$		$a\,^2T_1{}^{(2)}$	
$2\bar{A}$	$\frac{1}{2}u_+$	$-\frac{1}{2}u_-$	$\frac{1}{2}a_+$	$-\frac{1}{2}a_-$
$\frac{1}{2}u_+$	$\kappa_1+\frac{1}{2}g_s$			
$-\frac{1}{2}u_-$	0	$\kappa_1-\frac{1}{2}g_s$		
$\frac{1}{2}a_+$	$\kappa_3+\sqrt{2}k$	κ_4	$\kappa_2+k+\frac{1}{2}g_s$	
$-\frac{1}{2}a_-$	κ_4	$-\kappa_3+\sqrt{2}k$	0	$\kappa_2-k-\frac{1}{2}g_s$

linear combinations of $\frac{1}{2}u_+$ and $-\frac{1}{2}u_-$, and also $\frac{1}{2}a_+$ and $-\frac{1}{2}a_-$. Because of the form of the matrix, this leaves the two diagonal blocks unchanged.

$$\begin{aligned}|\tfrac{1}{2}\gamma_+\rangle' &= \cos\theta\,|\tfrac{1}{2}\gamma_+\rangle+\sin\theta\,|-\tfrac{1}{2}\gamma_-\rangle,\\ |-\tfrac{1}{2}\gamma_-\rangle' &= -\sin\theta\,|\tfrac{1}{2}\gamma_+\rangle+\cos\theta\,|-\tfrac{1}{2}\gamma_-\rangle,\end{aligned}\tag{23}$$

where $\gamma=u$ or a and $\tan2\theta=\kappa_4/\kappa_3$. After some algebra, we find

$$g_{\parallel}(2\bar{A})=2\{[\sin2\theta(\tfrac{1}{2}g_s\cos2\phi-k\sin^2\phi)]^2 +[\cos2\theta(\tfrac{1}{2}g_s+k\sin^2\phi)+\sqrt{2}k\sin^2\phi]^2\}^{1/2},\tag{24}$$

where

$$\tan2\phi=\frac{2}{\kappa_1-\kappa_2}\left[\kappa_3\cos\left(\arctan\frac{\kappa_4}{\kappa_3}\right)+\kappa_4\sin\left(\arctan\frac{\kappa_4}{\kappa_3}\right)\right],$$

and, in the trivial case $\kappa_3=\kappa_4=0$, $g_{\parallel}(2\bar{A})=g_s$. To a good approximation, at least for Cr^{3+} systems, a separation into orbital and spin parts can be made as follows:

$$g_{\rm orb}(2\bar{A})=\mathrm{sgn}(\sin2\phi)2k[(\sin^2\phi\cos2\theta+\sqrt{2}\sin2\phi)^2 +(\sin2\theta\sin^2\phi)]^{1/2},\tag{25}$$

$$g_{\rm spin}(2\bar{A})=2g_s(\tfrac{1}{4}\cos^2\!2\theta+\tfrac{1}{4}\sin^2\!2\theta\cos2\phi)^{1/2},\tag{26}$$

where ϕ is usually small so that $g_{\rm spin}\approx g_s$.

(ii) For $g_{\parallel}(\bar{E})$, we can neglect interactions with $a^2T_1\frac{1}{2}a_0$, i.e., set $\lambda_4=\lambda_5=0$ in Table III, since λ_2 is greater than λ_4 or λ_5. (The effect of doing this is shown in Sec. V.) This enables us to reduce the order of the $\bar{E}$ matrix from 3 to 2, which makes it easy to diagonalize analytically. Again, after some algebra we find

$$g_{\parallel}(\bar{E})=-g_s+2\sqrt{2}k\sin2\delta,\tag{27}$$

where $\tan2\delta=2\lambda_2/(\lambda_1-\lambda_3)$. The separation into orbital and spin parts is exact in this approximation.

For the calculation of $g_{\perp}(\bar{E})$, however, we cannot neglect the small interaction with $^2T_1\frac{1}{2}a_0$, as otherwise we find $g_{\perp}(\bar{E})=0$. The most satisfactory way to calculate $g_{\perp}$ is to diagonalize the zero-field 3×3 matrix for $\bar{E}$ and obtain eigenvector coefficients in the expansion

$$|a^2E\bar{E}\rangle=\alpha_1|a^2E-\tfrac{1}{2}u_+\rangle+\alpha_2|a^2T_1-\tfrac{1}{2}a_+\rangle +\alpha_3|a^2T_1\tfrac{1}{2}a_0\rangle.\tag{28}$$

Then,

$$(g_{\perp}\bar{E})=2(2\alpha_1\alpha_3-\alpha_2\alpha_3/\sqrt{2})k.\tag{29}$$

The definition of the order to which the g values have been calculated must be considered a little carefully. We are considering two perturbations on our zeroth-order Hamiltonian; a larger zero-field part, including off-diagonal Coulomb, trigonal field, and spin-orbit interactions (100–1000 cm^{-1}), and a much smaller Zeeman part (~1 cm^{-1}). By definition, a g value describes the linear part of the Zeeman splitting, i.e., it is of first order in the Zeeman perturbation. We have considered zero-field perturbations to second order—the diagonalization within $(a\,^2E^{(2)},a\,^2T_1{}^{(2)})$ does not really change the order, although we note that the admixture of $a\,^2T_1$ into $a\,^2E$ for Cr^{3+} systems is only ≈1–20% (i.e., $\sin\delta$, $\sin\phi$ is 0.1–0.4), so that almost another order has been added to the calculation. However, strictly, we should say that we have taken zero-field perturbations to second order and the Zeeman perturbation to first order. For those cases where v, $v'>\zeta$, one could reasonably drop the contributions quadratic in ζ.

C. Other Cubic Terms

The other cubic terms of interest, e.g., $a\,^2T_1$, $a\,^2T_2$, and $^4T_2$, interact with many more levels than $^4A_2$ and $a\,^2E$ and, consequently, analytical expressions for their g values become very complicated. In view of the limited number of systems for which these g values have been measured, it is better to calculate them numerically as described in Sec. III.

D. MD Intensities

The only MD transition from the ground state, which is allowed between the zeroth-order cubic terms, is $^4A_2\rightarrow{}^4T_2$. Thus, the dominant mechanism for allowing transitions to other excited $^{2S+1}\Gamma$ terms is the admixture of $^4T_2$ into $^{2S+1}\Gamma$. In all cases except $a\,^4T_1$ (where the trigonal field can also produce this mixing), the only perturbation which can produce the required admixture is spin-orbit coupling. The most important case to consider is the intensity of MD R lines ($^4A_2\leftrightarrow a\,^2E$) for Cr^{3+} ions in centrosymmetric sites. In zero magnetic field, there will in general be four R lines. This assumes that the small ground-state splitting $D(^4A_2)$ is resolved, but if it is not a summation over these components can be carried out. The above mechanism predicts equal absorption cross sections for each of the four lines when averaged over all polarizations

$$\tfrac{1}{3}\sum_{\kappa}\left(N^{-1}\int k_\sigma\,d\sigma\right)_{\kappa}(^4A_2\hat{\Gamma}_T;{}^2E\hat{\Gamma}_T')=\frac{1.27\times10^{-22}\eta\sigma\zeta^2k^2}{D_{14}{}^2}.\tag{30}$$

We note that to this order the trigonal field has no effect on the intensity. An equivalent expression was first obtained by Sugano *et al.*[3] [but note the absence of a factor h/m in their Eq. (9) and a factor of 3 in Eq. (10)]. In those cases where MD R lines have been observed in trigonal symmetry and the ground-state splitting resolved,[7,25] the spectra are averaged over all polarizations by the crystal geometry. It is observed that the four components do not have the same intensity [as would be predicted by the mechanism of Eq. (30)], the departure from equality being $\sim$20–30%. The mechanisms contributing to this asymmetry are numerous and of higher order than considered above. A number of these were calculated, but a satisfactory analytical expression could not be found. We, therefore, rely on numerical calculations for details of the intensity patterns. The absolute magnitude of the absorption cross section predicted by Eq. (30) is clearly very sensitive to the value of the energy denominator D_{14}. The zeroth-order value given in Table II can be up to a factor of 2 less than that measured or given by the exact-energy solution. If we take the latter value for D_{14}, the absolute absorption cross section given by Eq. (30) is still a factor of 2–10 higher than that given by the numerical solution (see Sec. V).

The situation for the B lines ($^4A_2 \rightarrow a\,^2T_2$) is not so straightforward. As there are two $\bar{E}$ components in $a\,^2T_2$, the zero-field perturbations must be diagonalized within $a\,^2T_2$, leading to much more complicated expressions than Eq. (30). We will not pursue this further but again rely on numerical calculations of these line strengths.

V. COMPARISON OF ANALYTICAL AND NUMERICAL METHODS AND RELATION TO EXPERIMENT

We will now compare the analytical solutions we have obtained with the "exact" numerical procedure outlined in Sec. III (and to which the analytical expressions are an approximation). To do this, we choose several examples of important Cr^{3+} impurity systems on which there are good optical data enabling the crystal-field parameters Δ, B, C, v, v', and ζ to be determined. The systems chosen are Al_2O_3:Cr^{3+} (ruby), $Be_3Al_2(SiO_3)_6$:Cr^{3+} (emerald), $ZnAl_2O_4$:Cr^{3+} (spinel) and MgO:Cr^{3+}. The case of $Y_3Al_5O_{12}$:Cr^{3+} (garnet) will be treated in more detail in a future publication. In addition to the above, we also briefly consider tetrahedrally coordinated Co^{2+} to explore the validity of the analytical expressions in a region where the Coulomb interaction is comparable to the cubic-field strength. The convergence of the perturbation expansion will clearly depend on the extent of the departure from the zeroth-order (strong cubic-field) approximation, i.e., it will depend on the values of off-diagonal Coulomb and trigonal-field matrix elements relative to the diagonal energy differences. The parameters describing most Cr^{3+} impurity systems are such that the expansion parameter is $\approx\frac{1}{3}$. This means that the convergence in these cases is reasonably good. The only really free parameters are those describing the crystal-field strength, i.e., Δ, v, and v', and Δ is fixed by the $^4T_2$ energy. The Coulomb (B and C) and spin-orbit (ζ) parameters are positive and are constrained to a small range about 20–30% below their free-ion values. Our philosophy on the orbital-reduction factor k is to use it as a slowly varying measure of the amount of covalency, and for Cr^{3+} systems we have kept it fixed at 0.7.

A. g Values

An inspection of Table IV shows that the perturbation expressions we have obtained for the g values of $^4A_2$ and $a\,^2E$ give a useful approximation to the numerical solution for Cr^{3+} ions in a range of environments. The values given by the analytical expressions [Eqs. (20), (21), (24), (27), and (29)] are listed in the row labeled "An." and the exact numerical solution is listed under "Num." In the case of $g_{\parallel}(^2E\bar{E})$, the result of diagonalizing the $3\times3\bar{E}$ matrix of Table III is given, the approximation of Eq. (27) being shown in parenthesis. This demonstrates the effect of neglecting interactions with $a\,^2T_1$ ($\frac{1}{2}a_0$). We see that, for the Cr^{3+} systems, the analytical and numerical methods agree within $\sim$50% in most cases, and the sign of the orbital contribution to the ^2E g values is given correctly. This is in contrast to the approximation of Sugano and Tanabe,[2] who considered only zero-field perturbations within t_2^3 and did not diagonalize these within $a\,^2E$, $a\,^2T_1$. For example, with the parameter values chosen in Table IV, their expression gives (for the orbital and spin contributions, respectively) $g_{\parallel}(^2E\bar{E})$ for ruby $=-0.214-2.002$ and, for Cr^{3+}: spinel, $g_{\parallel}(^2E\bar{E})$ $=-0.020-2.002$. We see that the orbital contribution for ruby is a factor of 3 low and for spinel is of the wrong sign and about two orders of magnitude low. Our present perturbation treatment has effected a substantial improvement. It should be noted that the sign of the orbital contribution to $g_{\parallel}(^2E)$ is different in different materials so that one cannot generalize about identifying the $2\bar{A}$ or $\bar{E}$ component by the magnitude of its g value. In Clogston's[23] calculation of $g_{\perp}(^2E\bar{E})$, he included most of the interactions with higher-lying levels to the order we have taken them here, but again did not diagonalize the perturbations within $a\,^2E$, $a\,^2T_1$. His results for ruby are about a factor of 2 larger than ours and a factor of 4 larger than the exact solution.

For very large departures from the zeroth-order approximation, the expansion parameter approaches unity and the perturbation expressions become unreliable. For example, for tetrahedral Co^{2+}, which is a fairly extreme case in that the energy separation between cubic terms is comparable with their coupling

[25] G. Burns, E. A. Geiss, B. A. Jenkins, and M. I. Nathan, Phys. Rev. **139**, A1687 (1965).

TABLE IV. A comparison of analytical and numerical calculations of g values and ZFS for some impurity systems, and a tabulation of the corresponding experimentally observed quantities. The g values are given as a sum of spin (the coefficient of g_s, =2.0023) and orbital (the coefficient of the orbital reduction factor k, taken as 0.7) parts. Only the $^4A_2$ and $a\,^2E$ terms are considered here. The $\sim$ sign indicates that the separation into spin and orbital components is not rigorous for the $2\bar{A}$ g values.

		$Al_2O_3:Cr^{3+}$ Ruby[a]	$Be_3Al_2(SiO_3)_6:Cr^{3+}$ Emerald[b]	$ZnAl_2O_4:Cr^{3+}$ Spinel[c]	$MgO:Cr^{3+}$ Cubic site[d]	$ZnO:Co^{2+}$ Tetradhdral Co^{2+}[e]
	An.	$0.9998g_s-0.0270k$ $=1.9829$	$0.9995g_s-0.0423k$ $=1.9717$	$0.9995g_s-0.0333k$ $=1.9781$	$0.9997g_s-0.0337k$ $=1.9780$	$0.9769g_s+0.3095k$ $=2.2038$
$g_{\parallel}\,{}^4A_2,\bar{E}$	Num.	$0.9998g_s-0.0271k$ $=1.9829$	$0.9998g_s-0.0423k$ $=1.9723$	$0.9998g_s-0.0315k$ $=1.9789$	$0.9998g_s-0.0337k$ $=1.9783$	$0.9933g_s-0.2656k$ $=2.2014$
	Expt	1.9840 ± 0.0006[f]	1.973 ± 0.002[g]	1.9807 ± 0.0001[h]	1.9797[i]	2.243 ± 0.001[j]
	An.	$0.9998g_s-0.0261k$ $=1.9835$	$0.9995g_s-0.0341k$ $=1.9776$	$0.9995g_s-0.0380k$ $=1.9748$		$0.9769g_s+0.3116k$ $=2.2055$
$g_{\perp}\,{}^4A_2,\bar{E}$	Num.	$0.9998g_s-0.0261k$ $=1.9835$	$0.9998g_s-0.0335k$ $=1.9784$	$0.9998g_s-0.0383k$ $=1.9751$	$=g_{\parallel}$	$0.9940g_s+0.2997k$ $=2.2301$
	Expt	1.9867 ± 0.0006[f]	1.97 ± 0.01[g]	1.9774 ± 0.0001[h]		2.2791 ± 0.0002[j]
	An.	$-1.000g_s-1.061k$ $=-2.741(-2.779)$	$-1.000g_s-1.882k$ $=-3.319$	$-1.000g_s+2.585k$ $=-0.189$	$-1.000g_s+0.155k$ $=-1.889$	$-1.000g_s+0.229k$ $=-1.624(-2.008)$
$g_{\parallel}a\,{}^2E,\bar{E}$	Num.	$-1.002g_s-0.942k$ $=-2.666$	$-0.994g_s-1.163k$ $=-2.804$	$-0.997g_s+3.129k$ $=0.195$	$-1.004g_s+0.227k$ $=-1.851$	$-0.897g_s-1.953k$ $=-3.358$
	Expt	-2.445 ± 0.001[k]	-2.71 ± 0.03[l]	0 ± 0.15[m]	$=-1.860\pm0.005$[n]	
	An.	$0.996g_s-1.152k$ $=1.205$	$0.999g_s-1.760k$ $=0.0770$	$0.995g_s+2.943k$ $=4.049$	$0.997g_s-0.2511k$ $=1.899$	$0.893g_s+2.534k$ $=3.689$
$g_{\parallel}a\,{}^2E,2\bar{A}$	Num.	$\sim0.99g_s-1.20k$ $=1.213$	$\sim1.02g_s-1.49k$ $=0.997$	$\sim1.01g_s+2.44k$ $=3.716$	$\sim1.00g_s-0.40k$ $=1.863$	$\sim0.88g_s+3.35k$ $=4.266$
	Expt	1.48[o]	$=1.04\pm0.02$[l]	1.85 ± 0.25[m]		
	An.	$0.128k=0.090$	$0.063k=0.044$	$0.087k=0.061$		$-0.847k=-0.677$
$g_{\perp}a\,{}^2E,\bar{E}$	Num.	$0.063k=0.044$	$0.492k=0.344$	$0.162k=0.113$	$=g_{\parallel}$[p]	$-1.333k=-1.066$
	Expt	0.0515 ± 0.0001[k]	0.27 ± 0.03[l]	0 ± 0.15[m]		
	An.	0.29[q]	1.55[q]	-1.52[q]	0	-3.37[q]
$D(^4A_2)$ $=-2D$	Num.	0.311	1.705	-1.712	0	-5.408
(cm^{-1})	Expt	0.3831[f]	$1.78\pm.07$[g]	-1.856 ± 0.001[h]	0	-5.5 ± 0.3[j]
$A(^2E)$	An.	-28.8[q]	99.0[q]	5.8[q]	0	-116.3[q]
$\bar{E}-2\bar{A}$	Num	-28.5	58.5	6.3	0	-90.3
(cm^{-1})	Expt	-29.14[o,f]	62.7[l]	6.72 ± 0.01[s]	0	

[a] For parameters $\Delta=18100$, $B=650$, $C=3120$, $v=800$, $v'=680$, $\zeta=180$ cm^{-1}.
[b] For parameters $\Delta=16200$, $B=780$, $C=2960$, $v=-2000$, $v'=2000$, $\zeta=225$ cm^{-1}.
[c] For parameters $\Delta=18250$, $B=700$, $C=3200$, $v=-200$, $v'=-1700$, $\zeta=250$ cm^{-1}.
[d] $\Delta=16600$, $B=650$, $C=3200$, $v=v'=0$, $\zeta=210$ cm^{-1}.
[e] For parameters $\Delta=4000$, $B=750$, $C=3500$, $v=400$ cm^{-1}, $v'=350$, $\zeta=450$ cm^{-1}.
[f] Reference 27.
[g] J. E. Geusic, M. Peter, and E. O. Shulz-duBois, Bell System Tech. J. **38**, 291 (1959).
[h] H. Kahan (private communication).
[i] J. E. Wertz and P. Auzins, Phys. Rev. **106**, 484 (1957).
[j] T. L. Estle and M. DeWitt, Bull. Am. Phys. Soc. **6**, 445 (1961).
[k] T. Muramoto, Y. Fukuda, and T. Hashi, J. Phys. Soc. Japan **26**, 1551 (1969).
[l] Reference 12.
[m] D. L. Wood, W. E. Burke, and L. G. Van Uitert, J. Chem. Phys. **51**, 1966 (1969).
[n] L. L. Chase, Phys. Rev. **168**, 341 (1968).
[o] S. Sugano and I. Tsujikawa, J. Phys. Soc. Japan **13**, 899 (1958).
[p] We find $g_{\parallel}(2\bar{A})=6.6251$, which departs from $3g_{\parallel}(\bar{E})$ by 0.4%, i.e., there should be two independent $g_{\parallel}$ values measurable for this system.
[q] Using the expression of Ref. 5.
[r] D. F. Nelson and M. D. Sturge, Phys. Rev. **137**, A1117 (1965).
[s] Reference 7.

via the Coulomb interaction, we find the situation in the last column of Table IV. In this case, the perturbation method ceases to be useful.

As we have already noted in Sec. IV, the g values of the other cubic terms are best calculated numerically because of the large number of interactions involved and the relatively slow convergence. The results of such a numerical calculation is given in Table V for the $a\,^2T_1$ and $a\,^2T_2$ terms. It will be seen that the departures from the first-order values [Eqs. (6.25) and (6.26) of Ref. 2] are appreciable in most cases. These g values are more difficult to measure than those of $a\,^2E$ because the linewidths are greater, but some measure of them can be obtained by high-pulsed field measurements[11] or magnetic circular dichroism.[26] They are also useful for identifying the transitions to these levels observed in excited-state absorption. The ZFS of $a\,^2T_1$ and $a\,^2T_2$ are also given in Table V for completeness and as an aid in identifying the levels. They are defined as follows (see also Fig. 1):

$$\delta_1{}^i=W(a\,^2T_i\bar{E}_b)-W(a\,^2T_i\bar{E}_a),$$
$$\delta_2{}^i=W(a\,^2T_i\bar{E}_a)-W(a\,^2T_i2\bar{A}). \qquad (31)$$

[26] K. Aoyagi, M. Kajiura, and M. Uesugi, J. Phys. Soc. Japan **25**, 1387 (1968).

TABLE V. g values and ZFS for the a^2T_1 and a^2T_2 terms. These are not amenable to a satisfactory analytical perturbation treatment. The results of numerical calculations are given here. Note the definitions of the ZFS given in the text.

			$Al_2O_3:Cr^{3+}$ Ruby-num.[a]	Ruby-expt	Emerald-num.[a]	Spinel-num.[a]	MgO:Cr^{3+} num.[a]
$^2T_1$	$g_{\parallel}$	$2\bar{A}$	$\sim 0.990g_s+3.221k$ $=4.233$	···	$\sim 1.141g_s+2.548k$ $=4.067$	$\sim 0.997g_s+0.041k$ $=2.020$	$\sim 0.996g_s+2.334k$ $=3.623$[b]
		$\bar{E}_a$	$0.952g_s+0.020k$ $=1.920$	···	$0.986g_s-0.108k$ $=1.899$	$-1.006g_s-0.548k$ $=-2.398$	$0.327g_s+.561k$ $=1.047$[b]
		$\bar{E}_b$	$-0.952g_s+3.053k$ $=0.230$	···	$-0.942g_s+2.535k$ $=-0.111$	$0.997g_s-0.086k$ $=1.936$	$-0.338g_s+1.367k$ $=0.280$
	$g_\perp$	$\bar{E}_a$	$0.976g_s+0.334k$ $=2.188$	···	$1.002g_s+0.496k$ $=2.354$	$0.177k=0.124$	$=g_{\parallel}$
		$\bar{E}_b$	$-0.025g_s+0.265k$ $=0.135$	···	$0.062g_s+0.034k$ $=0.148$	$0.998g_s-0.005k$ $=1.995$	
ZFS		δ_1^1	208.1	233[c]	816.0	550.8	57.2
(cm^{-1})		δ_2^1	−196.0	−211[c]	−765.1	111.5	0
$^2T_2$	$g_{\parallel}$	$2\bar{A}$	$\sim\lvert 0.999g_s-2.031k\rvert$ $=0.647$	0.69 ± 0.09[d]	$\sim\lvert 0.991g_s-1.244k\rvert$ $=1.114$	$\sim\lvert 1.011g_s-2.512k\rvert$ $=0.268$	$\sim\lvert 0.996g_s-2.110k\rvert$ $=0.519$[b]
		$\bar{E}_a$	$-0.993g_s-2.001k$ $=-3.389$	-2.97 ± 0.15[d]	$-1.016g_s-1.115k$ $=-2.815$	$0.996g_s+0.008k$ $=2.000$	$0.324g_s-0.647k$ $=0.177$[b]
		$\bar{E}_b$	$0.989g_s-0.009k$ $=1.974$	≈ 2[e]	$1.024g_s+0.031k$ $=2.072$	$-0.996g_s-2.397k$ $=-3.672$	$-0.350g_s-1.329k$ $=-1.631$
	$g_\perp$	$\bar{E}_a$	$-0.005g_s+0.263k$ $=0.174$	<0.6[d]	$-0.002g_s+0.158k$ $=0.107$	$1.000g_s-0.189k$ $=1.870$	$=g_{\parallel}$
		E_b	$0.995g_s+0.211k$ $=2.14$	···	$1.034g_s+0.051k$ $=2.106$	$0.010g_s+0.112k$ $=0.098$	
ZFS		δ_1^2	270.5	290[f]	1587.3	1515.5	94.0
(cm^{-1})		δ_2^2	108.1	75[f]	34.3	−501.9	0

[a] For parameter values, see Table IV.
[b] For the cubic sites in MgO, $2\bar{A}$ and $\bar{E}_a$ are degenerate as Γ_8. The difference in the g values for these components reflects the need for two independent g values for a Γ_8 level.
[c] J. Margerie, Compt. Rend. **255**, 1598 (1962).
[d] Reference 11.
[e] Reference 26.
[f] S. Sugano and I. Tsujikawa, J. Phys. Soc. Japan **13**, 889 (1958).

B. Nonlinear g Values

The most important nonlinear g value is that describing the interaction between the $\bar{E}$ and $2\bar{A}$ levels of $a\,^2E$ for $\mathbf{H}_\perp c$ axis. As we have already seen in Sec. II B, if $g_\perp(E)$ is negligible, the energies of the $\bar{E}$ and $2\bar{A}$ levels are given by an equation of the type (7), i.e., we expect the R line separation Λ to satisfy

$$\Lambda^2=\Lambda_0^2+(G_\perp\beta\mathbf{H})^2, \tag{32}$$

where Λ_0 is the separation at zero field. No splitting of the R lines occurs, but they show a nonlinear repulsion. Such nonlinear Zeeman effects have been observed in ruby[11] and emerald.[12] If the effect of $g_\perp(\bar{E})$ is not negligible, both $\bar{E}$ and $2\bar{A}$ levels will show a splitting in addition to their shifts, and we must diagonalize the matrix

$$\begin{pmatrix} \Lambda_0 & & & \\ 0 & \Lambda_0 & & \\ \frac{1}{2}G_\perp\beta H & 0 & 0 & \\ 0 & \frac{1}{2}G_\perp\beta H & \frac{1}{2}g_\perp\beta H & 0 \end{pmatrix}. \tag{33}$$

Typical values of $g_\perp$ are ~ 0.1, so this situation arises only for very sharp lines in high fields. For example, in ruby at the highest fields used by Aoyagi *et al.*[11] the splitting of the $\bar{E}$ level would be only $\sim\frac{1}{2}$ cm^{-1}, and, with the concentration of Cr^{3+} in their samples, the linewidth would mask this. The same is true of the emerald studies by Wood,[12] even though $g_\perp$ is larger giving a 3-cm^{-1} splitting at 200 kGaus. Table VI shows the result of numerical calculations of $G_\perp$ and a comparison with experiment for ruby and emerald—the only cases for which good data are available. There is a first-order spin contribution to $G_\perp$, so its value is close to 2. We note a small anomaly in the high-field Zeeman data for emerald, viz., the change in the R-line separation Λ-Λ_0 shows about a 10% departure from Eq. (32). This is shown also by better and more recent data by Wood.[27] The origin of this behavior is not clear at this stage.

For all practical purposes (at least for Cr^{3+} systems), the ground state can be described by a single g perpendicular, as noted in Eq. (8), i.e., the nonlinearity in the Zeeman splittings for $\mathbf{H}_\perp c$ is describable by a parameter directly related to $g_\perp$, and the energy of the four Zeeman components can be found from the solution of two 2×2 matrices by transforming to Zeeman quantization.[28] The departure from the relation (8) for tetrahedral Co^{2+} is noted in the footnote to Table VI.

C. MD Intensities and Lifetimes

We now restrict our attention to zero-phonon lines in centrosymmetric systems, such as spinels, garnets, and MgO, and use parity labels to emphasize that we are dealing with even-parity states. The only transition from the ground state which is allowed, between zero-order cubic terms, is $^4A_{2g}\rightarrow{}^4T_{2g}$, and this will have an

[27] D. L. Wood (private communication).
[28] E. O. Schulz-du Bois, Bell System Tech. J. **38**, 271 (1959).

TABLE VI. Nonlinear $G_\perp$ values for $^4A_2$ and ^2E terms for the same parameter values as in Table IV.

		$Al_2O_3:Cr^{3+}$ Ruby	$Be_3Al_2(SiO_3)_6:Cr^{3+}$ Emerald	$ZnAl_2O_4:Cr^{3+}$ Spinel	$ZnO:Co^{2+}$ Tetrahedral Co^{2+}
$^4A_2\,G_\perp(\bar{E}/2\bar{A})$	Num.	$\sim 1.7318g_s-0.0453k$ $=3.4358$[a]	$\sim 1.7317g_s-0.0579k$ $=3.4268$[a]	$\sim 1.7317g_s-0.0663k$ $=3.4209$[a]	$\sim 1.722g_s-0.515k$ $=3.8595$[b]
	Expt[c]	3.4364	3.417	3.4306	3.885
$^2E\,G_\perp(\bar{E}/2\bar{A})$	Num.	$\sim 0.998g_s-0.233k$ $=1.84$	$\sim 1.003g_s-0.321k$ $=1.83$	$\sim 0.998g_s-0.230k$ $=1.91$	$\sim 1.602g_s+0.805k$ $=3.77$
	Expt	1.70[d]	2.16[e]		

[a] These are equal to $\sqrt{3}g_\perp$ to 0.008% or better.
[b] Departs from $\sqrt{3}g_\perp$ by about 1.2%.
[c] Taken as $\sqrt{3}g_\perp$ (see Table IV).
[d] Reference 11.
[e] Reference 12, but see comments in text.

integrated absorption cross section per ion of $\sim 10^{-17}$ cm. The predominant mechanism for absorption to other $^{2S+1}\Gamma$ terms is the admixture of $^4T_{2g}$ into $^{2S+1}\Gamma$. The orthogonality of orbital states belonging to different representations of O_h makes the spin part of the MD operator $\mathfrak{y}=k\mathbf{L}+g_s\mathbf{S}$ ineffective in inducing transitions. The selection rules on components of $\mathfrak{y}$ are given in Table I. In the case of R line transitions, the absolute magnitude of the intensity is given within a factor of about 5 in most cases by the perturbation expression of Eq. (30), although, as we have noted already, the details of the R line intensity pattern almost always require numerical computation. As we can see from Eq. (30), there is an approximately inverse quadratic dependence of the intensity on the $^4T_{2g}$–$a\,^2E_g$ separation. Expressions equivalent to Eq. (30) for transitions to the $a\,^2T_{1g}$ and $a\,^2T_{2g}$ terms become rather unwieldy, and we have preferred to calculate them numerically.

The absolute measurement of the absorption cross section is complicated by two main factors. (i) In the case of impurity systems, which we have been discussing here, it is difficult to measure N, the number of absorbing centers/cm^3. This can be done either by calibrating absorption bands against the results of x-ray fluorescence or by a spin count using a calibrated EPR spectrometer. (ii) As a result of electron-phonon coupling, the intensity in the zero-phonon line is reduced. For weak coupling, such as that within the t_2^3 configuration, this reduction is given by e^{-S}, where S is a small quantity containing the electron-phonon coupling constant.[29] The rest of the intensity we can think of as being the MD part of the one-phonon sideband. This is, however, masked by the larger ED contribution to the sideband which arises from coupling to odd-parity phonons. Because of this, the calculated cross sections will tend to be higher than those observed by an amount which depends on the strength of the electron-phonon coupling. From the ratio of the sideband to zero-phonon intensity in ruby (where both are ED), it seems that, for the $a\,^2E$ level of Cr^{3+} systems, $e^{-S}\gtrsim 0.7$. It is, however, difficult to get an accurate measure of this. The effects outlined in (i) and (ii) above are least for the $^4A_{2g}$ and $a\,^2E_g$ terms, and we estimate that their effect on the absolute R line intensities introduces an uncertainty of about 50%. In addition, the MD transitions are very weak and, in lightly doped crystals, signal averaging must often be done to get a satisfactory signal-to-noise ratio.

A knowledge of the radiative lifetime $\tau_r(^4A_{2g},a\,^2E_g)$ also gives the absorption cross section from Eqs. (13) and (17), or (A2) and (A7). In practice, the determination of this lifetime for an isolated d^3 impurity is complicated by the presence of alternative modes of decay for the excited $a\,^2E_g$ levels. (i) Radiation occurs in the vibronic sidebands with a lifetime τ_s. The ratio τ_s/τ_r is given by the ratio of the integrated zero-phonon line intensity to that of the sideband, so this can be allowed for fairly reliably. (ii) Non radiative decay with lifetime τ_{nr} cannot be neglected for $a\,^2E$ relaxation and is completely dominant for every other excited state, with the possible exception of $^4T_{2g}$.

Neglecting pair effects which only become appreciable at high-impurity concentrations, the total lifetime τ can be written

$$\tau^{-1}=\tau_r^{-1}+\tau_s^{-1}+\tau_{nr}^{-1}. \tag{34}$$

In the case of ruby, Nelson and Sturge[30] were able to separate $(\tau_s^{-1}+\tau_{nr}^{-1})$ by measuring the lifetime under conditions of complete R line reabsorption. By using the ratio of R line to sideband intensity of 4.4,[31] we can determine the individual lifetimes of Eq. (34) from their data. The results are shown in Table VII, together with

TABLE VII. Experimental values of $a\,^2E\rightarrow{}^4A_2$ inverse lifetimes at 77°K.

	$\tau^{-1}(\text{sec}^{-1})$	$\tau_r^{-1}(\text{sec}^{-1})$	$\tau_s^{-1}(\text{sec}^{-1})$	$\tau_{nr}^{-1}(\text{sec}^{-1})$	Q
Ruby[a]	239±3	174±3	40±1	25±7	0.90
$MgO:Cr^{3+}$ [b]	86±1	9.9±2	25±5	52±10	0.40
$MgAl_2O_4:Cr^{3+}$ [c]	27.4±0.1	1.3±0.5	7.3±3	19±4	0.31
$ZnAl_2O_4:Cr^{3+}$ [d]	34.4±0.1	(4.2)	(11.2)	(19)	0.45

[a] From Ref. 30.
[b] From Ref. 31.
[c] From Ref. 7.
[d] τ^{-1} is from Ref. 7. The values given in parenthesis for τ_r^{-1} and τ_s^{-1} are obtained on the assumption that τ_{nr} is the same in the Zn and Mg spinels. This was done because there is no absorption data available on $ZnAl_2O_4:Cr^{3+}$ to determine τ_r^{-1}.

[29] M. H. L. Pryce, in *Phonons*, edited by R. W. H. Stevenson (Plenum Publishing Corp., New York, 1966), p. 403.

[30] D. F. Nelson and M. D. Sturge, Phys. Rev. **137**, A1117 (1965).

[31] G. F. Imbusch (private communication).

TABLE VIII. Integrated absorption cross sections [see Eqs. (13), (A2), (A3)] for MD transitions within the nominally t_2^3 levels. The refractive indices for spinel and MgO have been taken as 1.74.

A. $ZnAl_2O_4:Cr^{3+}$ [a]

$\frac{1}{3}\sum_k\left(\frac{1}{N}\int k_\sigma\, d\sigma\right)_\kappa \times 10^{22}$ cm

			$a\,^2E$		$a\,^2T_1$			$a\,^2T_2$		
			$2\bar{A}$	$\bar{E}$	$2\bar{A}$	$\bar{E}_a$	$\bar{E}_b$	$2\bar{A}$	$\bar{E}_a$	$\bar{E}_b$
	$2\bar{A}$	Num.	38.0	15.6	3.3	53.0	6.9	4.7	14.4	.03
		Obs.[b]	(29.5)	(18.0)						
$^4A_2$	$\bar{E}$	Num.	28.7	34.2	14.4	0.6	21.0	3.2	5.6	4.2
		Obs.[b]	(24.5)	(28.0)						

B. $MgO:Cr^{3+}$ [a] stress along [111]

$\left(\frac{1}{N}\int k_\sigma\, d\sigma\right)_\kappa \times 10^{22}$ cm

			$a\,^2E$		$a\,^2T_1$			$a\,^2T_2$		
			$2\bar{A}$	$\bar{E}$	$2\bar{A}$	$\bar{E}_a$	$\bar{E}_b$	$2\bar{A}$	$\bar{E}_a$	$\bar{E}_b$
	σ[d]	Num.	195	58.7	42.9	45.3	75.9	9.7	1.2	2.0
$^4A_2$[c]		Obs.[e]	128	79						
	π[d]	Num.	92.1	164.1	41.0	45.0	81.1	3.3	7.5	2.2
		Obs.[e]	79	128						

[a] For parameter values, see the footnotes to Table IV. For comments on the Mg spinel, see the accompanying text.
[b] These values were obtained from the lifetime τ_r^{-1} of Table VII. See footnote d of Table VII for additional comments.
[c] Since the ground-state splitting is not resolved optically under stress, we have summed over the ground-state components.
[d] The polarization of the incident light is defined with reference to the [111] direction as z axis. Thus, the σ spectrum ($E_{\perp z}, H_{\parallel z}$) has $\kappa = z$ and the π spectrum ($E_{\parallel z}, H_{\perp z}$) has $\kappa = x$.
[e] From Refs. 31 and 34. The sum of the $\bar{E}$ and $2\bar{A}$ cross sections is the average of absorption measurements on two samples. The relative intensities of the components under stress were obtained from the fluorescence data of A. L. Schawlow, A. H. Piksis, and S. Sugano, [Phys. Rev. **122**, 1469 (1961)]. Although the total cross sections are in very good agreement, the relative intensities in σ polarization are not so good. The reason for this is not known.

a similar analysis for $MgAl_2O_4:Cr^{3+}$ and $MgO:Cr^{3+}$. The values of τ_r are obtained directly from the R line-absorption measurements, τ_s/τ_r from the R line–to-sideband-intensity ratio, and τ from the fluorescence decay. We see that, for the $a\,^2E$ level in materials of comparable Debye temperature, the nonradiative part of the lifetime is about the same for all systems. If we define the quantum efficiency as $Q=(\tau_r^{-1}+\tau_s^{-1})/\tau^{-1}$, we see that, in the cases where the R line is MD, Q is substantially lower than in ruby.

In Table VIII, we give the results of a numerical calculation of the cross sections for absorption to $a\,^2E_g$, $a\,^2T_{1g}$ and $a\,^2T_{2g}$ for $ZnAl_2O_4:Cr^{3+}$, $MgAl_2O_4:Cr^{3+}$, and $MgO:Cr^{3+}$. The former includes and extends our recent work on Cr^{3+} spinels.[32] The calculated quantities for the Zn and Mg spinels are essentially the same. The experimental R line strengths for the Zn spinel are somewhat less reliable, as in the absence of absorption data they were obtained from the τ_r of Table VII which uses the assumption (which is probably very good) that τ_{nr} is the same for the Mg and Zn spinels. The relative strengths of the four R line components follow from the emission data of Wood *et al.*[7] This intensity pattern enables an assignment to be made of the relative ordering of the $^4A_2$ and $a\,^2E$ components. This is important, because the over-all cubic symmetry of the spinel structure prevents the observation of polarized transitions. The Mg spinel has strain-broadened R lines so that the ground-state splitting is not resolved. For $MgAl_2O_4:Cr^{3+}$, the measured absorption cross sections for R_1 and R_2 are 16×10^{-22} and 13×10^{-22} respectively, compared to calculated values from Table VIII of 54.0×10^{-22} and 49.8×10^{-22}. In view of this disagreement, it would be interesting to measure the R line absorption in the Zn spinel.

In $MgO:Cr^{3+}$, we have a good system to test our intensity calculations, because a very careful measurement of the R line-absorption cross section for Cr^{3+} ions in the cubic sites of MgO has recently been made by Imbusch[31] using two crystals with 7.0×10^{18} and 17.7×10^{18} Cr^{3+} ions/cm^3 in cubic sites. The number of Cr^{3+} ions was measured by Dravnieks and Wertz[33] using a calibrated EPR spectrometer. We have calculated the R line intensity for the $^4A_2\Gamma_8 \rightarrow {}^2E\Gamma_8$ transition and also for the case in which [111] stress is applied and the ^2E splitting is resolved. For the unstressed case, we find the total absorption cross section per ion $(N^{-1}\int k_\sigma\, d\sigma)_\kappa$ to be 2.55×10^{-20} cm, in very good agreement with the measurements of Imbusch[31] on two samples which yielded 2.3×10^{-20} and 1.8×10^{-20} cm, respectively. The calculated cross sections depend very little on the magnitude of the applied stress, as can be seen by comparing the total σ and π cross sections for levels which are degenerate in the absence of stress. A stress value of 20 kg/mm^2 was used in the calculation, i.e., $v=-15.4$, $v'=13.6$ cm^{-1}.[34] The $2\bar{A}$ and $\bar{E}_a$ levels of Table VIII arise from cubic Γ_8, $E_b(^2T_1)$ from Γ_6, and $E_b(^2T_2)$ from Γ_7. The label σ is used to denote the **H** vector of the

[32] Reference 7. In this paper, the calculated absolute oscillator strengths are a factor of 3 low due to a numerical error. The relative strengths are correct.

[33] S. Dravnieks and J. Wertz (private communication).
[34] R. M. Macfarlane, Phys. Rev. **158**, 252 (1967).

incident light $\parallel$ to [111] and π to denote the **H** vector $\perp$ to [111]. The ratios of the intensities of the R line components ($^4A_2 \rightarrow {}^2E2\bar{A} : {}^4A_2 \rightarrow {}^2E\bar{E}$) are 0.61 (obs.), 0.57 (calc.) for π polarization and 1.6 (obs.), 3.3 (calc.) for σ polarization. The origin of the discrepancy in the case of σ polarization is not known.

In view of the difficulty of obtaining a good absolute measurement of the absorption cross section and our inability at this stage to calculate the Condon factor e^{-S}, we consider the agreement between observed and calculated cross sections in Table VIII to be very satisfactory. This represents the first such detailed calculation of the MD absorption cross sections for transition-ion impurities. No further phenomenological parameters have been introduced in the intensity calculations, as we have used the values of the parameters determined by the zero-field energies.

VI. CONCLUSION

We have been concerned here with providing an analysis of the observed g values and MD line strengths for a number of d^3 impurity systems. By going beyond the usual analysis of energy levels, we are able to provide a more searching test of the assumptions of the parameterized crystal-field model, viz., that the impurity orbitals transform in the site group like d orbitals and that the vibronic coupling is small for the levels of interest. The parameters of the theory are well overdetermined by considering energies and ZFS together with g values and line strengths. We find, as we have done before,[35] that some of the apparent discrepancies between experiment and theory are removed by ensuring that the calculations are done completely and that any mathematical approximations made do not compromise the quantitative predictions of the model.

To this end we have also been concerned with the extent to which perturbation expressions for g values and MD line strengths, based on a strong cubic-field zeroth-order approximation, can provide an adequate approximation to the exact numerical solution within d^3 (exact in the sense that the perturbation series, if summed to infinity, would reproduce it). We find that previously published expressions are almost always inadequate. Where possible, these have been extended here to provide useful approximations. This is particularly true of the $^4A_2$ and $a\,{}^2E$ g values which are very important because the transitions involving these levels are sharp and their magnetic properties are well studied. Our analysis of g values has included the definition and calculation of nonlinear g values which are important when the Zeeman energy is comparable to the ZFS and the orbital and spin contributions to the g values have been given separately.

[35] R. M. Macfarlane, J. Chem. Phys. **42**, 442 (1965).

ACKNOWLEDGMENTS

The author wishes to thank Dr. G. Frank Imbusch for several helpful discussions on the subject of absorption cross sections and lifetimes and for his measurement of the R line absorption of MgO:Cr^{3+}. He would also like to thank S. Dravnieks and Professor J. Wertz for measuring the number of Cr^{3+} ions in the cubic sites of two samples of MgO:Cr^{3+}.

APPENDIX A

We present here some useful general expressions relating absorption cross sections, oscillator strengths, and radiative lifetimes to dipole matrix elements for a system of thermally populated electronic levels.

Consider a process involving absorption from a set $B_i{}^\alpha (i=1, \ldots m; \alpha=1, \ldots g_i)$ of m thermally populated levels with degeneracies g_i, to a set $A_j{}^\beta (j=1, \ldots n; \beta=1, \ldots p_i)$ of initially unpopulated excited states. Analogously to free-ion nomenclature[13] we call $^{2S+1}\Gamma$ a term, Γ_T a level, and γ_T a state, and the A's and B's can be interpreted as these crystal quantum numbers as appropriate. The line strengths for transitions from B_i to A for a given polarization κ are as follows:

$$\begin{aligned} \mathcal{S}_\kappa(A,B_i{}^\alpha) &= \sum_{j,\beta} |\langle A_j{}^\beta | D_\kappa | B_i{}^\alpha \rangle|^2, \\ \mathcal{S}_\kappa(A,B_i) &= \sum_\alpha \mathcal{S}_\kappa(A,B_i{}^\alpha), \\ \mathcal{S}_\kappa(A,B) &= \sum_i \mathcal{S}_\kappa(A,B_i), \quad \text{etc.} \end{aligned} \tag{A1}$$

The transition-dipole operator is denoted by **D**. In the case of MD transitions, $D_\kappa = (-eh/2mc)\sum_i (kl_i + g_s s_i)_\kappa$, where i labels individual electrons. It is also convenient to work with the quantity $\mathcal{S}_\kappa' = (2mc/eh)^2 \mathcal{S}_\kappa$, since $\mathcal{S}_\kappa'$ involves dimensionless matrix elements of the orbital and spin operators in units of h. We will obtain formulas for absorption cross sections in which the line strengths have been summed over all the substates of A. This summation can be trivially extended or restricted to include just those final states of interest. For example, if the final level is a cubic term, $A \equiv S, \Gamma$, if a Kramers doublet $A \equiv S, \Gamma, \hat{\Gamma}_T$, etc. Since the final state is unpopulated, there is no complication from Boltzmann factors in the summation. We can use Boltzmann statistics for the populations when we are dealing with an ensemble of independent absorbing centers.

The absorption cross section per ion for the process $B_i \rightarrow A$ for light with polarization κ is given by

$$\left(N^{-1}\int k_\sigma \, d\sigma\right)(A,B_i) = \frac{8\pi^3 \sigma \eta}{hc} \frac{N_i}{N g_i} \sum_\alpha \mathcal{S}_\kappa(A,B_i{}^\alpha), \tag{A2}$$

$$\left(N^{-1}\int k_\sigma \, d\sigma\right)(A,B_i) = \frac{\pi e^2 h \sigma \eta}{6m^2c^3} \frac{N_i}{N g_i} \sum_\alpha \mathcal{S}_\kappa'(A,B_i{}^\alpha), \tag{A3}$$

where

$$N_i/N=g_ie^{-\Delta_i/kT}/\sum_{i=1}^{m} g_ie^{-\Delta_i/kT},$$

and Δ_i is the energy of the ith level. To get the total cross section from all sublevels of B, we must sum (A2) over i. In the limiting cases $kT\gg\Delta_m$, i.e., all levels equally populated, and $kT\ll\Delta_2-\Delta_1$, i.e., only the lowest populated, the factor N_i/N takes the values $g_i/\sum_i g_i$ and $\delta_{1,i}$, respectively.

The oscillator strength is given by

$$f_\kappa(A,B_i)=\frac{8\pi^2mc\sigma}{he^2}\frac{N_i}{Ng_i}\sum_\alpha \mathcal{S}_\kappa(A,B_i{}^\alpha), \qquad \text{(A4)}$$

so that

$$f_\kappa=\frac{mc^2}{\pi e^2}\frac{1}{\eta}\left(N^{-1}\int k_\sigma\, d\sigma\right)_\kappa. \qquad \text{(A5)}$$

Now we consider the inverse process of radiation from a set of n thermally populated excited levels A_i in which the thermalization time is much faster than the radiative-decay time. In this case, the line strength is summed over all final states in B, so that we take account of all processes contributing to the radiative emptying of the excited levels. The quantity of interest is the averaged radiative lifetime which can be temperature-dependent if states are populated which have different line strengths to the ground levels. We find

$$\tau_r{}^{-1}(B,A)=\frac{64\pi^4\sigma^3\eta^3}{3h}\sum_j\frac{N_j'}{N'p_j}\sum_{\beta,\kappa}\mathcal{S}_\kappa(A_j{}^\beta;B). \qquad \text{(A6)}$$

This has been summed over j because it is assumed that the upper states have thermalized. If they are thermally isolated, each level can be treated separately as above, but in intermediate cases the situation is more complicated. The population factor is

$$\frac{N_j'}{N'}=p_j\,e^{-\Delta_j'/kT}/\sum_{j=1}p_i\,e^{-\Delta_j'/kT},$$

where Δ_j' measures the excitation energy above the lowest populated excited state. For $T\ll\Delta_2'-\Delta_1'$, only A_1 is populated and

$$\tau_r{}^{-1}(B,A_1)=\frac{64\pi^4\sigma^3\eta^3}{3h}\frac{1}{p_1}\sum_{\beta=1}^{p1}\sum_\kappa \mathcal{S}_\kappa(A_1{}^\beta;B). \qquad \text{(A7)}$$

To use the above expressions for ED transitions, set $\mathbf{D}=e\sum_\gamma\mathbf{r}_\gamma$ in (A1) and multiply (A2), (A6), and (A7) on the right-hand side by the factor $\rho=(1/\eta^2)(\epsilon_{\text{eff}}/\epsilon_0)^2$ and (A5) on the left-hand side by this same factor. [(A3) is not valid for ED as it involves $\mathcal{S}'$.] The dielectric-screening term $(\epsilon_{\text{eff}}/\epsilon_0)$ is discussed by Dexter.[36]

[36] D. L. Dexter, in *Solid State Physics*, edited by F. Seitz and D. Turnbull (Academic Press Inc., New York, 1958), Vol. 6, p. 353.

In the approximation of the Lorentz local-field correction (i.e., allowing for dipole-dipole terms), $\rho=[(\eta^2+2)/3\eta]^2$.

APPENDIX B

We give here the matrix elements of the zero-field perturbation operator $P=\mathcal{H}-H^{(0)}$ within $a\,{}^2E$, $a\,{}^2T_1$ to second order [see Eq. (23)]. These matrix elements have been denoted $\lambda_1\cdots\lambda_6$ and $\kappa_1\cdots\kappa_4$ in Table III.

$$\lambda_1=K-(\tfrac{2}{3}v^2+\tfrac{1}{2}\zeta^2+\tfrac{2}{3}\zeta v)/D_7-\tfrac{4}{3}\zeta^2/D_{14}-72B^2/D_{12}$$
$$-18B^2/D_{13}-v'^2/D_8-\tfrac{3}{2}\zeta^2/D_{10}-\tfrac{1}{6}\zeta^2/D_9-v'^2/D_{11},$$

$$\lambda_2=(\tfrac{1}{3}\sqrt{2}v^2+\tfrac{1}{3}\sqrt{2}\zeta v/+\tfrac{1}{4}\zeta^2)/D_7+\sqrt{2}\zeta^2/6D_{14}$$
$$+(3\sqrt{3}Bv'-\tfrac{1}{2}3\sqrt{2}B\zeta)/D_{13}-(\tfrac{1}{4}\sqrt{2}v'^2+\tfrac{1}{4}\zeta v'-3Bv')/D_8$$
$$-(-\tfrac{1}{4}\zeta v'+\tfrac{3}{2}\sqrt{2}B\zeta+\tfrac{1}{8}\sqrt{2}\zeta^2)/D_{10}$$
$$-(\tfrac{1}{4}\zeta v'+\zeta^2/24)/D_9+(\tfrac{1}{4}\sqrt{2}v'^2+\tfrac{1}{12}\zeta v')/D_{11},$$

$$\lambda_3=K-(\tfrac{1}{3}v^2+\tfrac{1}{3}\zeta v+\tfrac{1}{4}\zeta^2)/D_7-\tfrac{1}{12}5\zeta^2/D_{14}$$
$$-[\tfrac{3}{2}v'^2+\tfrac{1}{4}\zeta^2-\tfrac{1}{2}(\sqrt{6})v'\zeta]/D_{13}$$
$$-[(\tfrac{1}{4}\sqrt{2}v'+\tfrac{1}{4}\zeta-3B)^2+\tfrac{1}{8}\zeta^2]/D_8$$
$$-[(\tfrac{1}{4}\sqrt{2}v'+\tfrac{1}{4}\zeta+3B)^2+\tfrac{1}{8}\zeta^2)/D_{10}$$
$$-(\tfrac{1}{8}9v'^2+\tfrac{1}{8}\sqrt{2}v'\zeta+\zeta^2/48)/D_9$$
$$-(\tfrac{1}{8}v'^2+\sqrt{2}v'\zeta/24+\zeta^2/48)/D_{11},$$

$$\lambda_4=(\tfrac{1}{2}\zeta^2+\tfrac{1}{3}\zeta v)/D_7+\tfrac{1}{3}\zeta^2/D_{14}-3B\zeta/D_{13}+\tfrac{1}{4}\sqrt{2}\zeta v'/D_8$$
$$-(\tfrac{1}{4}\zeta^2+\tfrac{1}{2}\sqrt{2}\zeta v'+3\zeta B)/D_{10}-\tfrac{1}{12}\zeta^2/D_9+\tfrac{1}{12}\sqrt{2}\zeta v'/D_{11},$$

$$\lambda_5=-(\tfrac{1}{4}\sqrt{2}\zeta^2+\tfrac{1}{6}\sqrt{2}\zeta v)/D_7+\tfrac{1}{12}\sqrt{2}\zeta^2/D_{14}$$
$$-(-\tfrac{1}{2}\sqrt{3}\zeta v'+\tfrac{1}{4}\sqrt{2}\zeta^2)/D_{13}$$
$$-(\tfrac{1}{8}\zeta v'-\tfrac{1}{16}\sqrt{2}\zeta^2+\tfrac{3}{2}\sqrt{2}B\zeta)/D_8$$
$$-(\tfrac{1}{8}\zeta v'-\tfrac{1}{16}\sqrt{2}\zeta^2+\tfrac{3}{2}\sqrt{2}B\zeta)/D_{10}$$
$$-(\tfrac{1}{8}\zeta v'+\sqrt{2}\zeta^2/48)/D_9-(\zeta v'/24+\sqrt{2}\zeta^2/48)/D_{11},$$

$$\lambda_6=K-\tfrac{1}{2}\zeta^2/D_7-\tfrac{1}{3}\zeta^2/D_{14}-\tfrac{1}{2}\zeta^2/D_{13}$$
$$-[\tfrac{1}{8}\zeta^2+(\tfrac{1}{2}\sqrt{2}v'+3B)^2]/D_8$$
$$-[\tfrac{1}{8}\zeta^2+(\tfrac{1}{2}\sqrt{2}v'+3B)^2]/D_{10}-\zeta^2/24D_9-\zeta^2/24D_{11},$$

$$\kappa_1=K-(\tfrac{1}{3}2v^2-\tfrac{1}{3}2\zeta v+\tfrac{1}{2}\zeta^2)/D_7-4\zeta^2/3D_{14}$$
$$-72B^2/D_{12}-18B^2/D_{13}-v'^2/D_8-\tfrac{3}{2}\zeta^2/D_{10}$$
$$-\tfrac{1}{6}\zeta^2/D_9-v'^2/D_{11},$$

$$\kappa_2=K-(\tfrac{1}{3}v^2-\tfrac{1}{3}\zeta v+\tfrac{3}{4}\zeta^2)/D_7-\tfrac{1}{4}\zeta^2/D_{14}$$
$$-[\tfrac{3}{2}v'^2+\tfrac{1}{2}(\sqrt{6})\zeta v'+\tfrac{3}{4}\zeta^2]/D_{13}$$
$$-(\tfrac{1}{4}\sqrt{2}v'-\tfrac{1}{4}\zeta-3B)^2/D_8-(-\tfrac{1}{4}\sqrt{2}v'+\tfrac{1}{4}\zeta+3B)^2/D_{10}$$
$$-(\tfrac{1}{8}9v'^2-\tfrac{1}{8}\sqrt{2}v'\zeta+\tfrac{1}{16}\zeta^2/D_9$$
$$-(\tfrac{1}{8}v'^2-\sqrt{2}\zeta v'/24+\tfrac{1}{16}\zeta^2)/D_{11},$$

$$\kappa_3=-\sqrt{2}(-\tfrac{1}{3}v^2+\tfrac{1}{3}v\zeta+\tfrac{1}{4}\zeta^2)/D_7-\sqrt{2}\zeta^2/6D_{14}$$
$$+(3\sqrt{3}Bv'+\tfrac{3}{2}\sqrt{2}B\zeta)/D_{13}-v'(\tfrac{1}{4}\sqrt{2}v'-\tfrac{1}{4}\zeta-3B)/D_8$$
$$+\sqrt{2}\zeta(-\tfrac{1}{4}\sqrt{2}v'+\tfrac{1}{4}\zeta+3B)/2D_{10}+(\tfrac{1}{4}\zeta v'+\zeta^2/24)/D_9$$
$$-v'(-\tfrac{1}{4}\sqrt{2}v'+\tfrac{1}{12}\zeta)/D_{11},$$

$$\kappa_4=(-\zeta v+\tfrac{1}{2}\zeta^2)/D_7+\zeta^2/3D_{14}$$
$$-3B\zeta/D_{13}+(\tfrac{1}{4}\sqrt{2}\zeta v'-\tfrac{1}{12}\zeta^2)/D_9-\sqrt{2}\zeta v'/6D_{11}$$
$$-(-\tfrac{1}{4}\sqrt{2}v'\zeta+\tfrac{1}{4}\zeta^2+3B\zeta)/D_{10}.$$

The constant K occurs on all diagonal elements and may be ignored.